



Jefferys, K. M., M. G. Betts, W. D. Robinson, J. R. F. Curtis, T. A. Hallman, A. C. Smith, C. Strevens, and J. Aguirre-Gutiérrez. 2024. Breeding habitat loss linked to declines in Rufous Hummingbirds. *Avian Conservation and Ecology* 19(2):2. <https://doi.org/10.5751/ACE-02681-190202>
Copyright © 2024 by the author(s). Published here under license by the Resilience Alliance. Open Access. CC-BY 4.0

Research Paper

Breeding habitat loss linked to declines in Rufous Hummingbirds

Kendall M. Jefferys¹ , Matthew G. Betts² , W. Douglas Robinson³ , Jenna R. F. Curtis⁴ , Tyler A. Hallman^{3,5} , Adam C. Smith⁶ , Chloë Strevens⁷  and Jesús Aguirre-Gutiérrez^{1,8} 

¹Biodiversity and Earth Observation, Environmental Change Institute, School of Geography and the Environment, University of Oxford, Oxford, UK, ²Department of Forest Ecosystems and Society, Oregon State University, Corvallis, Oregon, USA,

³Department of Fisheries, Wildlife, and Conservation Sciences, Oregon State University, Oregon, USA, ⁴Cornell Lab of Ornithology, ⁵Bangor University, School of Environmental and Natural Sciences, ⁶Canadian Wildlife Service, Environment and Climate Change Canada, Ottawa, Ontario, Canada, ⁷University of Oxford, School of Geography and the Environment, Oxford, UK, ⁸Leverhulme Centre for Nature Recovery, University of Oxford, Oxford, UK

ABSTRACT. Habitat loss is the primary driver of biodiversity decline worldwide, but it remains unknown how land-cover change and, in general, habitat loss impact many migratory species, such as the Rufous Hummingbird (*Selasphorus rufus*). Here, we gathered 5115 occurrence records for the Rufous Hummingbird from professional and citizen-science data sets and parameterized species distribution models with four bioclimatic variables and two Landsat satellite spectral reflectance bands. We calculated the population change and change in the potential distribution of the Rufous Hummingbird across its breeding range in the Pacific Northwest of North America over the last 36 yr (1985–2021). Back-casting habitat suitability predictions over time, we provide the first quantifications of breeding habitat change for the Rufous Hummingbird, which has exhibited precipitous declines over the past two decades. Furthermore, we evaluated links between modeled habitat suitability, population abundance, and trends with a route-level analysis of Breeding Bird Survey data. We found notable habitat loss occurring in Bird Conservation Regions along the Pacific coast where the species is most abundant (54% and 34% decreases in suitable habitat area), with habitat loss in coastal regions linked to population decline. In contrast, we detected habitat gains in regions along the interior, northeastern edges of the breeding range (160% and 85% increases in suitable habitat area). However, increasing suitability does not guarantee species colonization of new habitat. Our results indicate the need to further investigate drivers of habitat loss, such as intensive forestry and suppression of early seral habitat, along the Pacific coast. Our modeling approach can be applied to efficiently detect and quantify habitat loss over time for a variety of taxa.

La perte d'habitat de nidification liée à la diminution des Colibris roux

RÉSUMÉ. La perte d'habitat est le principal facteur de déclin de la biodiversité dans le monde, mais on ne sait toujours pas comment les changements d'occupation du sol et, en général, la perte d'habitat affectent de nombreuses espèces migratrices, comme le Colibri roux (*Selasphorus rufus*). Dans le présent article, nous avons rassemblé 5115 mentions de Colibri roux tirées de jeux de données professionnelles et de science citoyenne, et nous avons paramétré les modèles de répartition de l'espèce au moyen de quatre variables bioclimatiques et de deux bandes spectrales du satellite Landsat. Nous avons calculé l'évolution de la population et la variation de la répartition potentielle du Colibri roux dans son aire de nidification sur la côte nord-ouest du Pacifique en Amérique du Nord, au cours des 36 dernières années (1985-2021). Par rétropélation des prévisions d'adéquation de l'habitat dans le temps, nous présentons les premières quantifications du changement de l'habitat de nidification du Colibri roux, qui a connu des diminutions accélérées au cours des deux dernières décennies. En outre, nous avons évalué les relations entre l'adéquation de l'habitat modélisé, l'abondance de la population et les tendances à l'aide d'une analyse à l'échelle des routes des données du Relevé des oiseaux nicheurs. Nous avons constaté une perte d'habitat importante dans les régions de conservation des oiseaux situées le long de la côte du Pacifique, où l'espèce est le plus abondante (54 % et 34 % de diminution de la superficie d'habitat adéquat), la perte d'habitat dans les régions côtières étant liée à la baisse de la population. En revanche, nous avons détecté des gains d'habitat dans les régions situées le long des limites intérieures et nord-est de l'aire de nidification (160 % et 85 % d'augmentation de la superficie d'habitat adéquat). Cependant, l'augmentation de l'adéquation ne garantit pas la colonisation par l'espèce d'un nouvel habitat. Nos résultats indiquent qu'il est nécessaire d'étudier plus en détail les facteurs de perte d'habitat, tels que la sylviculture intensive et l'élimination des milieux de début de succession, sur la côte du Pacifique. Notre approche de modélisation peut être appliquée pour détecter et quantifier efficacement la perte d'habitat dans le temps pour une variété de taxons.

Key Words: *climate change; habitat loss; land-cover change; remote sensing; Rufous Hummingbird; Selasphorus rufus; species distribution modeling*

INTRODUCTION

Globally, bird populations are facing increasing pressures of habitat loss and climate change (Langham et al. 2015, Bairlein 2016, Trautmann 2018), with rapid declines in avifauna evident across continents (Sodhi et al. 2004, Rosenberg et al. 2019, Burns et al. 2021). Beyond their intrinsic conservation values, declines in bird populations also threaten key ecosystem services, such as seed dispersal and pollination (Şekercioğlu et al. 2004). As one of the few families of avian pollinators, hummingbirds and their conservation are particularly important for maintaining diverse floral communities, with roughly 7000 species of plants in the Americas dependent on hummingbird pollination (Abrahamczyk and Kessler 2015). Currently, about 10% of the 366 known hummingbird species are considered threatened, and 60% of species exhibit declining populations (International Union for the Conservation of Nature (IUCN) 2020), suggesting further efforts are needed to conserve hummingbirds and the diversity of plants they pollinate.

The Rufous Hummingbird (*Selasphorus rufus*) has experienced a 65% population decline since the 1970s, with rates of decline accelerating nearly twofold from 2009–2019 (English et al. 2021). Drivers of these declines, however, are not well understood. Analysis of mark–recapture data from monitoring programs in British Columbia, Canada report that adult apparent survival for Rufous Hummingbirds was stable over the past 20 yr (1998–2017), suggesting juvenile recruitment or loss of quality breeding habitat may explain declines in population (Drake et al. 2022). Decreased juvenile survival has been suggested as a key driver of population declines for Neotropical migratory hummingbirds more broadly, including Rufous Hummingbirds (English et al. 2024). The longest-migrating hummingbird, Rufous Hummingbirds migrate from Mexico to breed in the Pacific Northwest (PNW) of the USA and British Columbia, Canada. Along southward migration routes, Rufous Hummingbirds forage on nectar-rich flowers and insects in high-altitude meadows (Rousseau et al. 2020). In their summer range, these hummingbirds tend to breed in shrubby habitats and forest openings (Healy and Calder 2020).

Forestry is a dominant land use in the PNW; on industrial lands, management is characterized by intensive practices that apply herbicides to reduce herbaceous and deciduous plant species, encouraging growth of select (often coniferous) tree species for timber (Betts et al. 2013). Meanwhile, federal lands are increasingly characterized by the dominance of closed-canopy coniferous forest after regional policy that limits clearcutting (Phalan et al. 2019). Given Rufous Hummingbird requirements for open, shrubby habitat and the floral resources provided within them (Healy and Calder 2020), prevailing forest management practices likely reduce the availability of breeding habitat. At the same time, climate change is expected to affect hummingbird populations by limiting floral resource availability, shifting hummingbird ranges and altering migration timing. Prieto-Torres and colleagues (2021), for example, predict that global change will reduce suitable habitat areas for the majority of resident hummingbirds in Mexico. Furthermore, periods of drought—which are expected to increase in severity in western North America under climate change (Wickham et al. 2023)—are known to reduce floral abundance, resulting in scarce food resources for hummingbirds (Brown and Kodric-Brown 1979).

Whereas a growing number of studies detect habitat loss as a function of conversion of one land-use type to another (e.g., forest to farmland; Hansen et al. 2013), quantifying the more subtle process of habitat loss due to forest degradation (i.e., change from an original forest type to a more simplified one) is more challenging—especially at the finer spatial scales that are necessary to inform management (Betts et al. 2022). Using Earth Observation and species distribution modeling approaches, we detect and quantify both habitat and population change for the Rufous Hummingbird over 36 yr. Here, we define habitat as the physical and biological conditions enabling actual or potential species occupancy of an area (Hall et al. 1997). We trained our model with raw spectral reflectance bands (instead of predefined land-cover categories) and climate variables, which allowed us to model species-specific habitat for the Rufous Hummingbird. This approach enabled us to address the following questions: (1) Where has the Rufous Hummingbird experienced habitat loss or gain since the 1980s? (2) How has the total extent of suitable breeding habitat changed over the past decades? (3) What is the relative importance of climate and spectral satellite data in determining the species distribution? (4) Does modeled habitat loss correlate to decreases in local Rufous Hummingbird abundance, based on independent data from the Breeding Bird Survey (BBS)? Furthermore, we used independent data from the Global Land Cover Land Use Change (GLCLU) data set to then investigate relationships between habitat suitability change and forest dynamics. Under the assumption that suitable habitat is linked to Rufous Hummingbird abundance, we expected to see the greatest levels of habitat loss on the Pacific coast where population declines are steepest (English et al. 2021). We also expected land cover to play a greater role in driving Rufous Hummingbird distributions than climate, given that forest degradation has been linked to avian declines in other regions (Betts et al. 2022).

METHODS

Study area

Our study focuses on the breeding range of the Rufous Hummingbird, which encompasses the Pacific Northwest (PNW) of North America. We focus here on breeding habitat change, as loss of quality breeding habitat has been suggested as a potential driver of population decline for this species (Moran and Fraser 2015, Drake et al. 2022). Spanning nine ecoregions, the PNW is an ecologically complex area influenced by large climatic and topographic gradients (Haugo et al. 2019) and characterized by high floral and faunal diversity (Hargrove and Hoffman 2004). The PNW can be divided into two distinct physiographic regions, with a moist forest zone falling west of the Cascade Mountain Range and drier forest located on the eastern side of the Cascades and southwestern Oregon (Gaines et al. 2022).

Bird survey data

We compiled information on hummingbird presences and absences from a combination of expert and citizen-science data sets. Species data were acquired from the Oregon 20/20 data set for the state of Oregon and from eBird for the remainder of the breeding range. For species distribution modeling, we included point-count data on Rufous Hummingbird presences and absences from the Oregon 20/20 project (Robinson et al. 2020a). In an effort to create a replicable benchmark for Oregon bird

distributions and abundance, professional ornithologists conducted stationary counts in over 20,000 georeferenced locations across the state of Oregon, with an additional 50,000 locations surveyed by professionals and citizen scientists. Between 2011–2019, surveys were conducted during the breeding season from 15 May to 10 July. Point-count locations were selected along accessible roads and trails using a stratified random sampling scheme. Analysis of the habitat composition around survey points indicated the survey design sampled habitats in direct proportion to those present across the whole state (Robinson et al. 2020a). Counts were 5 min long with an unlimited distance radius.

To facilitate modeling across the full breeding range, we downloaded eBird stationary count data (eBird Basic Dataset 2022), filtered to closely match Oregon 20/20 survey protocol. eBird is a semistructured citizen-science project with flexible survey protocols and methods to account for variations in observer effort (Johnston et al. 2021). Observers submit eBird observations in the form of a checklist that includes information on species detected, location and date of observation, distance traveled, survey protocols, etc. From eBird, we obtained Rufous Hummingbird detections in “complete” checklists over 6 yr (2013–2019) to match the years of available Landsat 8 imagery and the Oregon 20/20 data collection period. Complete checklists in eBird mean that all species were recorded, which allows for zero-filling to generate presence–absence data. We included complete checklists submitted from May through July and geographically filtered observations to those within the breeding range study area we defined in Google Earth Engine (GEE), based on eBird range maps. Observer efforts can vary widely, so we removed checklists with greater than 10 observers, as recommended best practice (Johnston et al. 2021).

We elected to combine the Oregon 20/20 and eBird data sets because the Oregon 20/20 data set is less susceptible to spatial and temporal biases common to citizen-science data (Strimas-Mackey et al. 2020), and the eBird data set allowed us to fully cover the known species breeding range. Furthermore, combining expert and citizen-science survey data may improve model accuracy, as different survey structures capture complementary information on species occurrences (Robinson et al. 2020b).

Spatial thinning and class balancing

In both data sets, Rufous Hummingbird prevalence was low (<10%). Modeling distributions of rare species creates class imbalance, as non-detections heavily outweigh detections (Robinson et al. 2018). Following Steen et al. (2021), we first spatially thinned both Oregon 20/20 and eBird data, keeping one presence and absence point per 250 m pixel. Absence points were then spatially undersampled to roughly the sample size of the presences. After spatial thinning and subsampling, we had 5115 presence points and 4716 absence points from the combined Oregon 20/20 and eBird data sets for model construction.

Selection of predictor variables

Spectral remote sensing data

Recent scientific work has highlighted the ability of raw, atmospherically corrected remote-sensing data in species distribution models (SDMs) to detect fine-scale change in species habitat (Betts et al. 2022) and increase model accuracy (Shirley et al. 2013, Hopkins et al. 2022). In these “reflectance” models,

red and near-infrared bands account for most of the predictive power, suggesting that some information is lost when raw bands are classified into indices such as normalized difference vegetation index (NDVI) or land-cover categories (Shirley et al. 2013). However, raw spectral bands may also introduce multicollinearity, which must be addressed depending on model algorithm and research objectives.

We assessed multicollinearity of explanatory covariates with pairwise correlations (Append. 1 [Figs. S1.1, S1.2 and S1.3]). Five of the six reflectance bands (red, blue, green, swir1, and swir2) were highly collinear (Pearson’s $r > 0.65$). Random Forest is a non-parametric algorithm, well-suited to handling highly correlated data sets (Svetnik et al. 2003), but extrapolating to the past or future assumes the structure of collinearity does not change over time (Dormann et al. 2013). Considering the main purpose of our model was to back-cast and detect habitat change over time, we elected to include only red and near-infrared spectral bands, which were not collinear. For modeling, median spectral surface reflectance was taken from Landsat 8 OLI/TIRS collection 2 Tier 1 imagery over the months of May, June, and July from 2013–2019.

Selection of climate predictors

We selected climate variables from the TerraClimate data set due to its relatively high spatial resolution (ca. 4 km) and better suitability for temporal analysis compared with WorldClim (Abatzoglou et al. 2018). TerraClimate contains monthly climate and water balance on terrestrial surfaces from 1985 and is updated annually. We selected minimum and maximum temperature as well as the Palmer Drought Severity Index (PDSI) to characterize temperature and precipitation, known to drive hummingbird distributions (Vásquez-Aguilar et al. 2021; Appendix 1 [Fig S1.2]). Precipitation accumulation was correlated to maximum temperature (Pearson’s $r > 0.65$), so we instead selected PDSI, a measure of relative dryness (Dai 2011). Our final selected remote sensing and climate variables did not exhibit collinearity (Pearson’s $r < 0.65$; Appendix 1 [Fig S1.3]).

We included maximum wind speed at 10 m, a fairly novel predictor in avian distribution modeling. Wind stress (exposure + speed) is an overlooked yet important predictor for plant species occurrence (Momberg et al. 2021), suggesting wind may be valuable in modeling other species distributions. Wind speed may also affect avian distributions by influencing insect abundance and foraging effort. For instance, Barn Swallows (*Hirundo rustica*) have lower breeding success and adult body mass in years with windy summers, likely due to reduced insect abundance and foraging ability (Møller 2013). Rufous Hummingbirds aerially forage for insects, key sources of protein, vitamins, and fatty acids in hummingbird diets (Moran et al. 2019). Therefore, high wind speeds during the breeding season could be particularly detrimental to nesting success, as female Rufous Hummingbirds exhibit increased insect foraging when provisioning nestlings (Moran et al. 2019).

Species distribution models

Following methodology outlined in Betts et al. (2022), we implemented a species distribution model (SDM) using Landsat surface reflectance and climate variables as predictors. The combination of spectral remote sensing and climate data has been shown to improve model performance and predictive ability (Vila-

Viçosa et al. 2021). For each predictor, we summarized the summer median value over time at the 250 m scale, capturing typical breeding season conditions. Nearest neighbor resampling, the default method in GEE, was used when reducing resolution. The SDM was trained with data averaged from 2011–2019, then back-cast annually to quantify habitat suitability over the past decades. Our SDM was back-cast to every year since 1985, the beginning of Landsat imagery and TerraClimate data. All modeling was conducted on the GEE platform following a reproducible workflow for SDMs in GEE developed by Crego et al. (2022).

Model implementation and habitat change detection

We implemented a presence-absence SDM for the Rufous Hummingbird using the Random Forest classifier (“smileRandomForest”) in GEE. Random Forest is a machine-learning classification approach in which the probability of a classification is determined by a series of decision trees, also referred to as binary recursive partitioning (Guisan et al. 2017). For training and testing data, summer median values for climate and remote-sensing predictors were taken from 2013–2019 at the 250 m scale for presence and absence points. Median predictor values at presence and absence points were exported for model tuning with the “caret” package in R to select parameters that resulted in the highest accuracy based on area under the curve (AUC) evaluation. Our subsequent model contained 3000 decision trees, two variables per tree split, and a maximum leaf node per tree of 362. The model was assessed with tenfold cross-validation, with 80% of the data reserved for training, 20% reserved for testing. To reduce spatial autocorrelation, we separated training and testing data by spatial blocking with 200 km² grid cells. Model performance was assessed by the AUC value, which ranges from 0 to 1. An AUC of 0.5 indicates the model performed no better than random, whereas a value of one indicates perfect model fit (Fielding and Bell 1997). We provide further accuracy metrics, including the True Skill Statistic (TSS), omission (FNR) and commission rates (FPR) in Append. 1 (Table S1).

To back-cast model predictions annually, red and near-infrared spectral bands from Landsat imagery and climate bands from TerraClimate were averaged over summer months for each year over the 1985–2021 period. To get annual mosaics from Landsat imagery, cloudy pixels were masked and the median image was taken for the summer months. Bands from Landsat 7 ETM+ and Landsat 5 TM were harmonized with transform coefficients developed by Roy et al. (2016). We then applied our model classifier to yearly images with combined spectral and climate bands. We excluded the year 2012 from our model predictions, as there were large gaps in satellite imagery during this year due to errors in Landsat 7 ETM+.

To identify areas of significant change in habitat suitability over the full time period, we applied the GEE function “FormaTrend” to the image collection of annual habitat suitability predictions. “FormaTrend” fits a linear regression at the pixel level over the entire time series (36 yr), generating an image raster with the slope of the linear regression over each pixel and a *t*-test statistic to assess significance of trends. To quantify total habitat area over time, we masked annual habitat suitability images with the average classification threshold (habitat suitability > 0.42) that maximizes

the sum of sensitivity and specificity, and calculated the image area in square kilometers. Therefore, we consider “habitat” as an area where habitat suitability is above our classification threshold and “habitat loss” as any area previously classified as habitat that has fallen below this suitability threshold. Because annual habitat area was highly variable, likely due to interannual variations in climatic conditions (Append. 1 [Fig. S1.5]), percent change in habitat area over time was quantified by comparing 6-yr median images in the past (1985–1990) to the present (2016–2021). Percent change in area was then calculated for the four main Bird Conservation Regions (BCRs) intersecting the Rufous Hummingbird breeding range: the Northern Pacific Rainforest, Northwestern Interior Forest, Northern Rockies, and Great Basin. Bird Conservation Regions are ecoregions with overlapping bird communities, habitats, and management concerns; spatial data on BCRs was obtained from Bird Studies Canada and North American Bird Conservation Initiative (NABCI) (2014).

To explore spatial overlap between forest disturbance and Rufous Hummingbird habitat suitability change, trends in habitat suitability over the 2000–2021 period were estimated with a linear regression at the pixel level using the GEE function FormaTrend, as described above. These short-term trends in habitat suitability allowed for spatial analysis of the percent area overlap of hummingbird habitat suitability change and forest disturbance, extent loss, or gain. Forest types were derived from the GLCLU forest dynamics data set (2000–2020).

Habitat suitability effects on Breeding Bird Survey population trends, abundance

North American BBS data were used to assess whether habitat suitability could predict Rufous Hummingbird abundance and population trends from an independent data set. This provided another form of validation for our SDM. Beginning in 1966, BBS is an annual survey of breeding birds in North America, conducted along a set of 40 km routes. Trained observers stop at 50 regularly spaced intervals for 3-min point counts of every bird observed within 400 m. Employing a hierarchical negative binomial regression model, we estimated the effect of habitat suitability and changes in suitability over time on the relative abundance and population trends of Rufous Hummingbirds at BBS routes. Route-level trends and abundance estimates from BBS data allowed us to link local predictor values at route locations with route-specific observations, while adjusting for the differences in observer skill levels and sampling variation commonly employed in BBS models (e.g., Sauer and Link 2011).

To model effects of habitat suitability on population trends and abundance, we estimated annual habitat suitability for the area surrounding each BBS route from 1985–2021. We calculated the mean habitat suitability for every year, within a 200 m buffer of each BBS route on which the species has been observed and for which we had GIS information on the route’s path (Patuxent Wildlife Research Center 1999, Environment and Climate Change Canada 2023). For each route, we then estimated the mean suitability and an average rate of change in suitability over time using a linear regression and used these route-level estimates as predictors on the intercept and slopes of a hierarchical Bayesian negative binomial regression model of the BBS counts on each

route. This BBS model estimated the mean counts (route-level intercepts) and changes over time in mean counts (route-level trends) at each BBS route, while adjusting for effects common in the BBS data. These effects include variation in mean counts among observers, the first-year start-up effect common in BBS data (Kendall et al. 1996), and residual variation in abundance and trend not explained by habitat suitability. We also ran the model separately for two different time periods, because the BBS broad-level trend estimates suggest a possible change point in the species' population trends in approximately 2005. For a complete description of the BBS model and all data and code to replicate the analyses, see Appendix. 2.

RESULTS

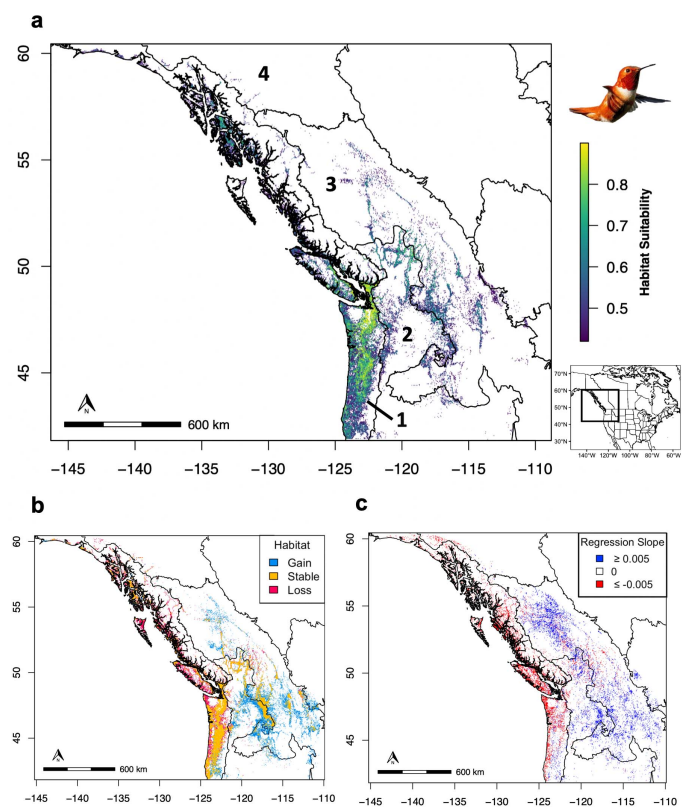
Overall, our SDM obtained a mean AUC of 0.81 (standard deviation: 0.03) when tested on independent, spatially blocked data. This indicates reliable prediction for Rufous Hummingbird distributions. Our model predicted highly suitable habitat along the Pacific coast in Washington, Oregon, and British Columbia (Fig. 1a), consistent with existing breeding range and abundance maps (Fink et al. 2022). Measures of variable importance suggested that Rufous Hummingbird distributions are primarily driven by minimum temperature, followed by the red surface reflectance band, maximum temperature, drought severity, near-infrared surface reflectance, and maximum wind speeds, respectively (Fig. 2). The median minimum summer temperature was 9.8°C in the 250 m around presence points and 8.1°C for absence points (Append. 1 [Fig. S1.6b]). The median maximum temperature was 22.4°C for presence points compared with 23.8°C for absence (Append. 1 [Fig. S1.6a]).

Habitat extent and change over time

Comparing the 6-yr median classified habitat suitability images (habitat suitability > 0.42) from the past (1985–1990) with the present (2016–2021), we detected clear regional patterns of habitat change for Rufous Hummingbirds. Habitat loss was concentrated in coastal regions (Fig. 1b), such as the Northern Pacific Rainforest BCR, with a loss of 59,166 km² of suitable habitat area where the species is most abundant during breeding (Fink et al. 2022; Fig. 3). Meanwhile, we detected habitat gain to the northeastern portion of the Rufous Hummingbird breeding range (Fig. 1b).

Although suitable habitat area over the entire breeding range increased by 13% overall, strong geographic patterns in habitat change indicated that these metrics may be better understood when broken into more regional geographies, such as BCRs. Quantifying change in habitat area by BCR (Table 1) revealed 34% declines in suitable habitat area in the Northern Pacific Rainforest BCR, which covers core areas of the Rufous Hummingbird breeding range. In contrast, BCRs located in the northern and eastern edges of the breeding range, such as the Northern Rockies and Great Basin BCRs, showed substantial percent increases in suitable habitat area (160% and 85%, respectively). Habitat suitability trends, based on a pixel-level linear regression on annual suitability values across the 36-yr time period, showed the same regional split as changes in total habitat area. We found significant negative annual rates of change ($\beta \leq -0.005$, $df(35) = -2.03$, $\alpha = 0.05$) in habitat suitability occurring

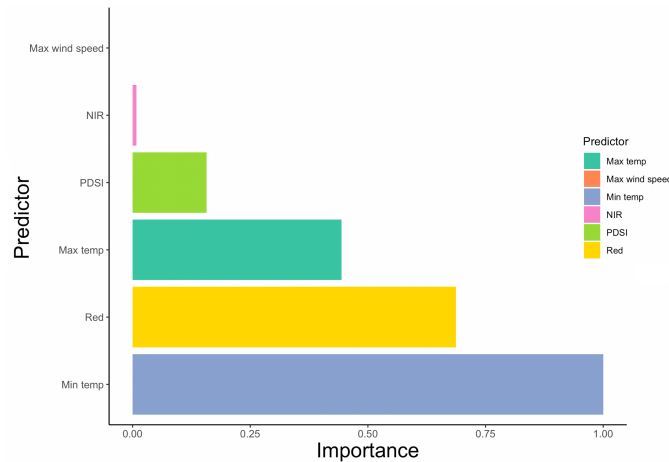
Fig. 1. (a) Predicted habitat distribution of the Rufous Hummingbird (*Selasphorus rufus*) in its summer breeding range. (b) Comparison of habitat area between a 6-yr median of past predictions (1985–1990) and present (2016–2021). Areas classified as habitat in past predictions but not in present predictions are considered habitat loss (pink). Areas classified as habitat in the present but non-habitat in the past are considered habitat gain (blue). Areas classified as habitat in both images are considered stable habitat (yellow). (c) Significant trends in habitat suitability as detected by the slope of the linear regression on a pixel-by-pixel basis across each year in the 36-yr time period. Negative slopes along the coast (red) and positive slopes to the east (blue) reveal regional variation in habitat trends. Maps show Bird Conservation Region (BCR) boundaries (labeled in panel (a)): 1. Northern Pacific Rainforest, 2. Great Basin, 3. Northern Rockies, 4. Northwestern Interior Forest) rather than the state and province boundaries shown in the map inset.



along the Pacific coast, west of the Cascade Range, and significant positive annual rates of change ($\beta \geq 0.005$, $df(35) = 2.03$, $\alpha = 0.05$) east of the Cascades (Fig. 1c).

Quantifying area overlap of forest dynamic layers from the GLCLU data set and habitat suitability trends revealed links between forest disturbance and habitat suitability. Compared with pixels of increasing or stable habitat suitability, pixels with declining habitat suitability generally had a higher proportion of forest gain (Fig. 4). However, the majority of pixels with declining habitat suitability

Fig. 2. Mean variable importance values from tenfold random forest model runs, values standardized 0–1, where larger values suggest a higher importance of the variable for determining the distribution of the species.

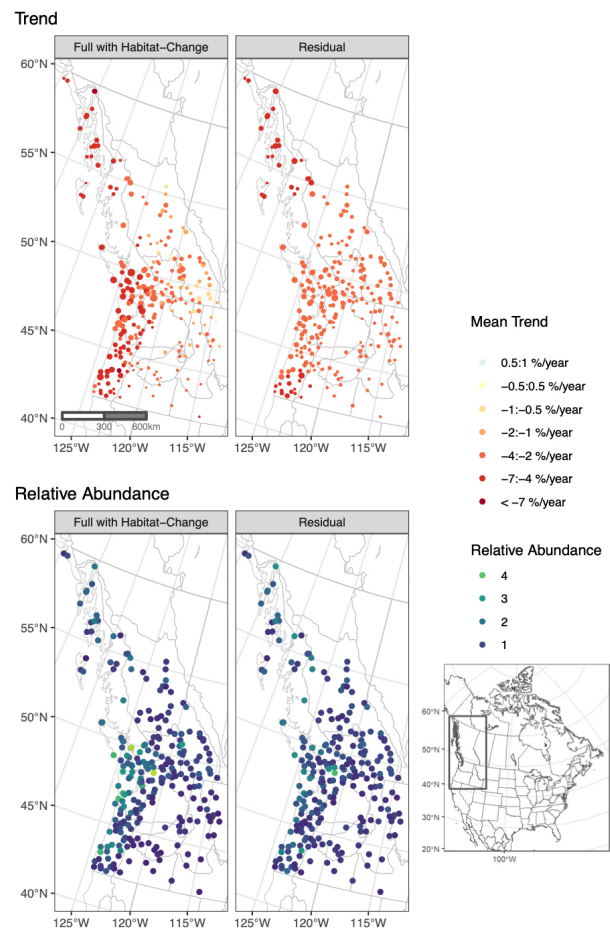


occurred in stable forest (Fig. 4). Stable forest in the GLCLU data set is characterized by no detected changes in canopy cover or forest structure (height), changes that would be indicative of forest extent loss or disturbance from stand replacement. In contrast, pixels with increasing habitat suitability had a higher proportion of forest disturbance or loss, especially in the core breeding areas located with the Northern Pacific Rainforest BCR, suggesting Rufous Hummingbirds may respond positively to some level of forest disturbance (Fig. 4). This association of increasing habitat suitability and forest disturbance is not as strong for the Great Basin and Northern Rockies BCRs, where there is a much higher overlap of increasing habitat suitability with non-forest areas (Fig. 4).

Habitat suitability effects on Breeding Bird Survey abundance and population trends

According to BBS data, Rufous Hummingbird populations declined steeply after the year 2005. Between the years 2006 and 2021, our BBS model estimated an overall change in the population of approximately -43% [-52–33], with the steepest rates of decline in the Pacific coastal regions where the species is also most abundant (Fig. 3). Over this time period, the effect of change in the habitat suitability on trends (P_β) was clearly positive, such that routes with modeled declines in habitat suitability had more negative population trends ($P_\beta = 0.025$ [0.0028–0.048]). The greater declines in habitat suitability in the coastal region accounts for most of the increased rates of decline in that region (Fig. 3); the residual trend component alone (Fig. 3, right panel) does not show the same coastal-decline pattern. The effect of mean habitat suitability (P_α) on mean relative abundance was strong and positive (effect of mean habitat suitability, $P_\alpha = 3$ [2.2–3.8]). Results were similar for the first 20 yr of the BBS trend analyses (1985–2005); Routes with greater habitat suitability had higher mean abundance ($P_\alpha = 3.1$ [2.3–4.0]) and routes with greater declines in habitat suitability generally had more negative population trends, although the 95% credible interval overlapped zero ($P_\beta = 0.05$ [-0.011–0.11]). Detailed results for this earlier time-period are included in supplementary materials (Append. 2).

Fig. 3. Map of the trends for the Rufous Hummingbird from 2006–2021. The colors represent the trends in abundance for BBS routes in the upper panel and the relative abundance of BBS routes in the lower panel. The left panel represents the full estimated trends and abundance on each route, including both the effect of habitat suitability and the residual component not related to habitat. The right panel represents the trends and relative abundances after removing the effect of habitat suitability. In the top-left panel, the greater declines in coastal regions are evident from the darker red points compared with the top-right panel. In the bottom-left panel, the higher abundance near the coast is evident from the lighter colors. The bottom-right panel shows much more even relative abundance across the species' range, showing that habitat suitability accounts for much of the variation in abundance.



DISCUSSION

Rufous Hummingbirds have exhibited concerning rates of population decline over the past decades, rates that have accelerated since the early 2000s. As drivers of this decline were largely unknown, we sought to understand where, and to what extent, breeding habitat loss for the species was occurring. Between 1985 and 2021, we detected substantial habitat loss in coastal regions (Northern Pacific Rainforest and Northwestern

Table 1. Percent change in Rufous Hummingbird habitat area by Bird Conservation Region (BCR). Habitat area data come from our 6-yr medians of habitat suitability for the beginning and end of the study time period. Percent change in habitat area over time was quantified by comparing total area of suitable habitat of 6-yr median images of habitat suitability in the past (1985–1990) to the present (2016–2021) as seen in Fig. 1b.

BCR [†]	Habitat area 1985–1990 (km ²)	Habitat area 2016–2021 (km ²)	Percent change (%)
Northern Pacific Rainforest	173404.23	114238.1	-34
Great Basin	35765.11	66038.77	85
Northern Rockies	38706.78	100768.92	160
Northwestern Interior Forest	1461.41	682.93	-53

[†] Three BCRs were omitted from this table (Prairie Potholes, Southern Rockies/ Colorado Plateau, and Badlands and Prairies) as they fall on the eastern fringes of the Rufous Hummingbird breeding range; however, the small areas of these regions that did overlap with the breeding range experienced increases in suitable habitat area.

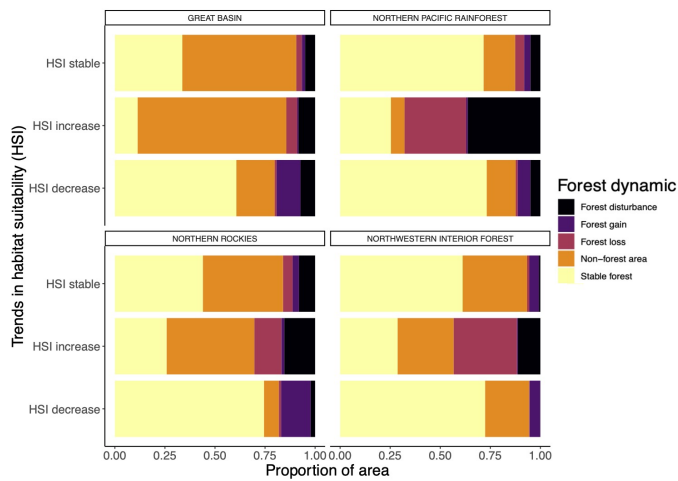
Interior Forest BCRs) where Rufous Hummingbirds are most abundant (Healy and Calder 2020; Fig. 3) and where populations exhibit the steepest declines (English et al. 2021; Fig. 3).

The strong, positive effect of mean habitat suitability on BBS route-level abundance further validated our SDM predictions, suggesting that modeled habitat suitability is linked to local measures of hummingbird abundance. The positive effect of habitat suitability change on BBS population trends since 2005, after which populations declined steeply, indicates that declines in breeding habitat suitability are linked to Rufous Hummingbird declines. Furthermore, the geographic patterns of high population decline in core breeding range areas support that population declines are driven by habitat conditions on the breeding grounds. If population declines were occurring primarily in the non-breeding range or during migration, we would expect to see steeper population declines on the periphery of the breeding range and a more stable core breeding range as remaining individuals concentrate in areas of more suitable habitat conditions.

Minimum summer temperature, red spectral reflectance, and maximum summer temperature were highly important predictors in our model. First considering climate, minimum summer temperature had the highest variable importance, highlighting potential sensitivity of Rufous Hummingbirds to rising summer temperatures. In the PNW, climate models predict increases in temperature ranging from 2.0 to 2.6°C by the timeframe of 2036–2065 (Vose et al. 2017), with the highest temperature increases predicted for summer months in this region (Mote et al. 2013). Differences in mean temperature of presence and absence points in our SDM suggest that 1–2°C increases in summer temperatures would affect habitat suitability (Append. 1 [Fig. S1.6a,b]). Based on these estimates, we would expect future rising of mean summer temperatures to increase habitat suitability to the northeast and reduce habitat suitability on the warmer Pacific coast.

Rising minimum temperature may underlie increasing availability of suitable habitat on the northeastern edges of the breeding range, such as the Great Basin and Northern Rockies BCRs. In these regions, we see a large proportion of both habitat suitability

Fig. 4. Rufous Hummingbird habitat suitability change over time (2000–2021) by forest dynamic class from the GLCLU data set (2000–2020), split by the four main BCRs in the Rufous Hummingbird breeding range. Area of stable habitat includes any 250 m pixel where the slope of the linear regression on habitat suitability values were between -0.007 and 0.007. Area of habitat suitability loss includes pixels where the regression slope was less than -0.007 and area of habitat suitability gain includes pixels where the regression slope was greater than 0.007. This threshold indicated a significant change in habitat suitability based on a two-sided *t*-test of the long-term habitat suitability trend against the time series of pixel values.



increases and decreases occurring in stable forest or non-forest areas, further supporting evidence that increases in habitat suitability to the northeast of the Rufous Hummingbird breeding range are likely driven more by changes in climate variables than forest dynamics or vegetation cover captured by spectral bands (Fig. 4). This shift is consistent with reports of Rufous Hummingbirds expanding their breeding range farther into the northeast, interior region of British Columbia (Moran and Fraser 2015) and, more broadly, previous work documenting bird range shifts northward due to climate change (Thomas and Lennon 1999, Hitch and Leberg 2007, Lehikoinen and Virkkala 2016). Although modeling approaches may predict species range shifts in response to a changing climate, species dispersal and ability to colonize new habitat area is less certain. The use of mechanistic models (as in Fordham et al. 2021) could lend insight into species potential to colonize increasingly suitable habitat to the northeast. However, quantitative data on natal and breeding dispersal of Rufous Hummingbirds are limited.

Raw spectral bands can capture fine-scale changes in vegetation health and cover not captured in broad land cover or vegetation type categories, such as changes in forest composition, age, and responses to different disturbance types and plant stress (Negrón-Juárez et al. 2020, Betts et al. 2022). Our use of raw spectral reflectance bands allowed us to detect forest degradation through changes in forest age and composition (Betts et al. 2024) in our models, where lack of forest disturbance may be the primary factor driving declines in habitat suitability (Fig. 4). Previous work suggests Rufous Hummingbirds frequently inhabit disturbed forests, both post-fire

and post-harvest (Hutto 1995, Hutto and Young 1999), potentially benefiting from increases in floral resources following disturbance from logging or fire (Korpela et al. 2015, Mola and Williams 2018). We found positive associations between habitat suitability trends and forest disturbance, suggesting Rufous Hummingbirds may respond positively to some level of forest disturbance. Increased human population density has also been linked to declines in survival rates of adult and juvenile Rufous Hummingbirds in their breeding range (English et al. 2024), potentially aligning with our own findings, as we would expect that with greater human population density there is more suppression of natural disturbances, such as fire.

The majority of habitat suitability declines we detected occurred in areas of stable forest cover, suggesting either that habitat suitability may decrease over time when there is a lack of forest disturbance and/or that climate plays a larger role in driving habitat loss than land-cover change. Considering the former, habitat suitability declines in stable forest may be explained by succession on federal lands after the Northwest Forest Plan limited clearcutting on federal lands in the early 1990s, with previously early seral stands undergoing succession to become denser, closed-canopy stands (Phalan et al. 2019). In tandem with succession on federal lands, recent intensification of forestry in the PNW has likely reduced floral resources and the quality of early seral forest habitat on industrial lands. Previous work in this region has found negative associations between avian species richness, including Rufous Hummingbird abundance, and intensive forestry practices such as herbicide use (Betts et al. 2013, Kroll et al. 2017).

Importantly, our results do not imply that old-growth forests lack quality habitat for Rufous Hummingbirds. Rather, we suggest that the dominance of mid-seral forest due to histories of fire suppression and policies promoting old-growth forest (Donato et al. 2020) may explain ongoing declines in habitat suitability in landscapes with stable forest cover. Compared with early successional stages and old-growth, mid-seral successional stages are associated with lower bird diversity (Schieck and Song 2006). As forests mature into old-growth stands, canopy gaps allow for greater floral abundance and arthropod availability (Franklin et al. 2002). Indeed, previous work documents associations between Rufous Hummingbirds and old-growth forests when there are light gaps in the canopy allowing for sufficient floral resources (British Columbia Conservation Data Centre 2015).

Estimates of forest cover loss can improve estimates of habitat loss and extinction risk from deforestation (Tracewski et al. 2016); however, our analysis for the Rufous Hummingbird exemplifies how suitability models built with raw spectral bands can better detect habitat loss due to forest degradation. This was found in previous work using SDMs based on raw spectral satellite data, which linked avian declines to forest degradation in areas of stable canopy cover (Betts et al. 2022). Species distribution models built with raw spectral bands have been shown to more accurately predict habitat compared with predefined categories of land-cover change (Shirley et al. 2013, Oeser et al. 2020). This has important conservation implications for habitat loss and extinction risk metrics. For instance, in the absence of population

trends, IUCN Red List criteria often rely on assessments of habitat loss based on predefined land-cover categories, such as forest cover (IUCN 2012), which may not accurately reflect species habitat needs.

Accuracy metrics indicated that our model runs performed well when tested on spatially blocked hold-out data. However, we note that our model was validated with predictors averaged over multiple years, which may not fully capture model ability to predict suitability based on annual predictor values. We also recognize that forest dynamics data from the GLCLU data set were available only over the last two decades, rather than the full study time period. This may be a limited window in which to examine forest dynamics in this region, considering widespread changes in the forestry practices in the USA following the passage of the 1994 Northwest Forest Plan (Thomas et al. 2006). It is possible that we might be seeing a decline in Rufous Hummingbirds due to unprecedently high habitat levels as a result of heavy logging in the 1960s–1980s without herbicide use, which may have temporarily increased foraging resources.

Migratory species face varied pressures throughout their ranges and along migration pathways, complicating efforts to understand drivers of decline and the impacts of habitat loss. In this study, we identified breeding habitat loss as a likely factor in Rufous Hummingbird population declines. Our findings underscore the risk of continued habitat degradation to Rufous Hummingbirds and the need to better understand and address land-use practices, such as intensive forestry and suppression of natural disturbance agents, that may reduce suitable breeding habitat. Although breeding habitat loss has been identified as a main driver of population declines of other migratory birds (Hallworth et al. 2021), long-distance migrants, such as Rufous Hummingbirds, are likely exposed to various threats across large geographic scales. For instance, land-use change may reduce quality stopover sites along hummingbird migration routes, and climate change may alter plant phenology, linked to migration timing (López-Segoviano and Arenas-Navarro 2018).

The changes we detected in potential breeding range distribution have concerning implications for Rufous Hummingbird populations under increasing temperatures and continued land-use change. We encourage future research examining Rufous Hummingbird response to forest management, particularly how different types of disturbances affect hummingbird abundance, juvenile recruitment, and breeding habitat quality (i.e., floral resources and nesting success). We also recommend future work quantifying habitat change in the non-breeding range and migratory stop-over sites for comparison with breeding range habitat trends. Such work would provide a fuller understanding of threats throughout Rufous Hummingbird life cycles and identify priority areas for conservation efforts. The framework for habitat change analysis we present here has broader conservation applications, as this work can be extended not only to better understand the extent and effects of habitat loss for Rufous Hummingbirds but also for other species of conservation concern across the globe.

Author Contributions:

KMJ, MGB, JAG, and CMS contributed to conceiving and refining the idea. WDR, JRC, TAH collected Oregon occurrence data. KJM led all habitat analyses with input from JAG and MGB. ACS and KJM co-led the BBS modeling with input from MGB. KJM drafted the manuscript. All authors contributed to editing and refining the final manuscript.

Acknowledgments:

We thank all the volunteers who have participated in BBS data collection. Thanks to Dr. Ramiro Crego for technical advice and for publishing excellent tutorials online on running SDMS in GEE. Dr. Josée Rousseau kindly provided input on filtering eBird data for modeling. The Hummingbird Conservation Workshop, organized by Dr. Susan Bonfield, provided valuable context on the key threats to western hummingbirds. KJM received scholarship and support from the Rhodes Trust. JAG was funded by the Natural Environment Research Council (NERC; NE/T011084/1) and the Oxford University John Fell Fund (10667). This material is based partly upon work supported by the H.J. Andrews Experimental Forest and Long Term Ecological Research (LTER) program under the NSF grant LTER8 DEB-2025755.

Data Availability:

All code and data used in the BBS analyses are available at https://github.com/AdamCSmithCWS/Jefferys_etal. All Google Earth Engine code and data for species distribution modeling are available at https://code.earthengine.google.com?accept_repo=users/kendalljefferys30/Jefferys_Manuscript_RUHUSDM_HabitatChange.

LITERATURE CITED

Abatzoglou, J. T., S. Z. Dobrowski, S. A. Parks, and K. C. Hegewisch. 2018. TerraClimate, a high-resolution global dataset of monthly climate and climatic water balance from 1958–2015. *Scientific Data* 5: 170191. <https://doi.org/10.1038/sdata.2017.191>

Abrahamczyk, S., and M. Kessler. 2015. Morphological and behavioural adaptations to feed on nectar: how feeding ecology determines the diversity and composition of hummingbird assemblages. *Journal of Ornithology* 156:333–347. <https://doi.org/10.1007/s10336-014-1146-5>

Bairlein, F. 2016. Migratory birds under threat. *Science* 354: 6312. <https://doi.org/10.1126/science.aah6647>

Betts, M. G., J. Verschuyt, J. Giovanini, T. Stokely, and A. J. Kroll. 2013. Initial experimental effects of intensive forest management on avian abundance. *Forest Ecology and Management* 310:1036–1044. <https://doi.org/10.1016/j.foreco.2013.06.022>

Betts, M. G., Z. Yang, A. S. Hadley, J. Hightower, F. Hua, D. Lindenmayer, E. Seo, and S. P. Healey. 2024. Quantifying forest degradation requires a long-term, landscape-scale approach. *Nature Ecology Evolution* 8:1054–1057. <https://doi.org/10.1038/s41559-024-02409-5>

Betts, M. G., Z. Yang, A. S. Hadley, A. C. Smith, J. S. Rousseau, J. M. Northrup, J. J. Nocera, N. Gorelick, and B. D. Gerber. 2022. Forest degradation drives widespread avian habitat and population declines. *Nature Ecology Evolution* 6:709–719. <https://doi.org/10.1038/s41559-022-01737-8>

Bird Studies Canada and North American Bird Conservation Initiative (NABCI). 2014. Bird conservation regions. Bird Studies Canada on behalf of the North American Bird Conservation Initiative, Port Rowan, Ontario, Canada. <https://birdscanada.org/bird-science/nabci-bird-conservation-regions>

British Columbia Conservation Data Centre. 2015. Species summary: *Selasphorus rufus*. British Columbia Ministry of Environment, Victoria, British Columbia, Canada. <https://a100.gov.bc.ca/pub/eswp/>

Brown, J. H., and A. Kodric-Brown. 1979. Convergence, competition, and mimicry in a temperate community of hummingbird-pollinated flowers. *Ecology* 60:1022–1035. <https://doi.org/10.2307/1936870>

Burns, F., M. A. Eaton, I. J. Burfield, A. Klvaňová, E. Šilarová, A. Staneva, and R. D. Gregory. 2021. Abundance decline in the avifauna of the European Union reveals cross-continental similarities in biodiversity change. *Ecology and Evolution* 11:16647–16660. <https://doi.org/10.1002/ece3.8282>

Crego, R. D., J. A. Stabach, and G. Connette. 2022. Implementation of species distribution models in Google Earth Engine. *Diversity and Distributions* 28:904–916. <https://doi.org/10.1111/ddi.13491>

Dai, A. 2011. Characteristics and trends in various forms of the Palmer Drought Severity Index during 1900–2008. *Journal of Geophysical Research* 116(D12): 115. <https://doi.org/10.1029/2010JD015541>

Donato, D. C., J. S. Halofsky, and M. J. Reilly. 2020. Corraling a black swan: natural range of variation in a forest landscape driven by rare, extreme events. *Ecological Applications* 30: e02013. <https://doi.org/10.1002/eap.2013>

Dormann, C. F., J. Elith, S. Bacher, C. Buchmann, G. Carl, G. Carré, J. R. G. Marquéz, B. Gruber, B. Lafourcade, P. J. Leitão, T. Münkemüller, C. McClean, P. E. Osborne, B. Reineking, B. Schröder, A. K. Skidmore, D. Zurell, and S. Lautenbach. 2013. Collinearity: a review of methods to deal with it and a simulation study evaluating their performance. *Ecography* 36:27–46. <https://doi.org/10.1111/j.1600-0587.2012.07348.x>

Drake, A., C. Bishop, A. Moran, and S. Wilson. 2022. Geographic and temporal variation in annual survival of a declining neotropical migrant hummingbird (*Selasphorus rufus*) under varying fire, snowpack, and climatic conditions. *Frontiers in Ecology and Evolution* 10: 825026. <https://doi.org/10.3389/fevo.2022.825026>

eBird Basic Dataset. Version: EBD_relJun-2022. Cornell Lab of Ornithology, Ithaca, New York, USA.

English, S. G., C. A. Bishop, S. Wilson, and A. C. Smith. 2021. Current contrasting population trends among North American hummingbirds. *Scientific Reports* 11: 18369. <https://doi.org/10.1038/s41598-021-97889-x>

English, S. G., S. Wilson, Q. Zhao, C. A. Bishop, and A. J. Moran. 2024. Demographic mechanisms and anthropogenic drivers of contrasting population dynamics of hummingbirds. *Biological Conservation* 289: 110415. <https://doi.org/10.1016/j.biocon.2023.110415>

Environment and Climate Change Canada. 2023. North American breeding bird survey: Canadian trends website, data, version 2023. Environment and Climate Change Canada, Gatineau, Quebec, Canada.

Fielding, A. H., and J. F. Bell. 1997. A review of methods for the assessment of prediction errors in conservation presence/absence models. *Environmental Conservation* 24:38-49. <https://doi.org/10.1017/S0376892997000088>

Fink, D., T. Auer, A. Johnston, M. Strimas-Mackey, S. Ligocki, O. Robinson, W. Hochachka, L. Jaromczyk, A. Rodewald, C. Wood, I. Davies, and A. Spencer. 2022. eBird status and trends, data version: 2021; released: 2022. Cornell Lab of Ornithology, Ithaca, New York, USA. <https://doi.org/10.2173/ebirdst.2021>

Fordham, D. A., S. Haythorne, S. C. Brown, J. C. Buettel, B. W. Brook. 2021. poems: R package for simulating species' range dynamics using pattern-oriented validation. *Methods in Ecology and Evolution* 12:2364-2371. <https://doi.org/10.1111/2041-210X.13720>

Franklin, J. F., T. A. Spies, R. V. Pelt, A. B. Carey, D. A. Thornburgh, D. R. Berg, D. B. Lindenmayer, M. E. Harmon, W. S. Keeton, D. C. Shaw, K. Bible, and J. Chen. 2002. Disturbances and structural development of natural forest ecosystems with silvicultural implications, using Douglas-fir forests as an example. *Forest Ecology and Management* 155:399-423. [https://doi.org/10.1016/S0378-1127\(01\)00575-8](https://doi.org/10.1016/S0378-1127(01)00575-8)

Gaines, W. L., P. F. Hessburg, G. H. Aplet, P. Henson, S. J. Prichard, D. J. Churchill, G. M. Jones, D. J. Isaak, and C. Vynne. 2022. Climate change and forest management on federal lands in the Pacific Northwest, USA: managing for dynamic landscapes. *Forest Ecology and Management* 504: 119794. <https://doi.org/10.1016/j.foreco.2021.119794>

Guisan, A., W. Thuiller, and N. E. Zimmermann. 2017. Habitat suitability and distribution models: with applications in R. Cambridge University Press, Cambridge, UK. <https://doi.org/10.1017/9781139028271>

Hall, L. S., P. R. Krausman, and M. L. Morrison. 1997. The habitat concept and a plea for standard terminology. *Wildlife Society Bulletin (1973-2006)* 25:173-182.

Hallworth, M. T., E. Bayne, E. McKinnon, O. Love, J. A. Tremblay, B. Drolet, J. Ibarzabal, S. van Wilgenburg, and P. P. Marra. 2021. Habitat loss on the breeding grounds is a major contributor to population declines in a long-distance migratory songbird. *Proceedings of the Royal Society B: Biological Sciences* 288: 20203164. <https://doi.org/10.1098/rspb.2020.3164>

Hansen, M. C., P. V. Potapov, R. Moore, M. Hancher, S. A. Turubanova, A. Tyukavina, D. Thau, S. V. Stehman, S. J. Goetz, T. R. Loveland, A. Kommareddy, A. Egorov, L. Chini, C. O. Justice, and J. R. G. Townshend. 2013. High-resolution global maps of 21st-century forest cover change. *Science* 342:850-853. <https://doi.org/10.1126/science.1244693>

Hargrove, W. W., and F. M. Hoffman. 2004. Potential of multivariate quantitative methods for delineation and visualization of ecoregions. *Environmental Management* 34:S39-S60. <https://doi.org/10.1007/s00267-003-1084-0>

Haugo, R. D., B. S. Kellogg, C. A. Cansler, C. A. Kolden, K. B. Kemp, J. C. Robertson, K. L. Metlen, N. M. Vaillant, and C. M. Restaino. 2019. The missing fire: quantifying human exclusion of wildfire in Pacific Northwest forests, USA. *Ecosphere* 10: e02702. <https://doi.org/10.1002/ecs2.2702>

Healy, S., and W. A. Calder. 2020. Rufous Hummingbird (*Selasphorus rufus*), version 1.0. Birds of the World. <https://doi.org/10.2173/bow.rufhum.01>

Hitch, A. T., and P. L. Leberg. 2007. Breeding distributions of North American bird species moving north as a result of climate change. *Conservation Biology* 21:534-539. <https://doi.org/10.1111/j.1523-1739.2006.00609.x>

Hopkins, L. M., T. A. Hallman, J. Kilbride, W. D. Robinson, and R. A. Hutchinson. 2022. A comparison of remotely sensed environmental predictors for avian distributions. *Landscape Ecology* 37:997-1016. <https://doi.org/10.1007/s10980-022-01406-y>

Hutto, R. L. 1995. Composition of bird communities following stand-replacement fires in northern Rocky Mountain (U.S.A.) conifer forests. *Conservation Biology* 9:1041-1058. <https://doi.org/10.1046/j.1523-1739.1995.9051033.x>

Hutto, R. L., and J. S. Young. 1999. Habitat relationships of landbirds in the Northern Region, USDA Forest Service (No. RMRS-GTR-32). U.S. Department of Agriculture, Forest Service, Rocky Mountain Research Station, Fort Collins, Colorado, USA. <https://doi.org/10.2737/RMRS-GTR-32>

International Union for the Conservation of Nature (IUCN). 2020. The IUCN red list of threatened species. IUCN Biodiversity Assessment and Knowledge Team: Red List Unit, Cambridge, UK. <https://www.iucnredlist.org/en>

IUCN. 2012. IUCN red list categories and criteria, version 3.1, second edition. IUCN, Gland, Switzerland.

Johnston, A., W. M. Hochachka, M. E. Strimas-Mackey, V. Ruiz Gutierrez, O. J. Robinson, E. T. Miller, T. Auer, S. T. Kelling, and D. Fink. 2021. Analytical guidelines to increase the value of community science data: an example using eBird data to estimate species distributions. *Diversity and Distributions* 27:1265-1277. <https://doi.org/10.1111/ddi.13271>

Kendall, W. L., B. G. Peterjohn, and J. R. Sauer. 1996. First-time observer effects in the North American breeding bird survey. *Auk* 113:823-829. <https://doi.org/10.2307/4088860>

Korpela, E.-L., T. Hyvönen, and M. Kuussaari. 2015. Logging in boreal field-forest ecotones promotes flower-visiting insect diversity and modifies insect community composition. *Insect Conservation and Diversity* 8:152-162. <https://doi.org/10.1111/icad.12094>

Kroll, A. J., J. Verschuy, J. Giovanini, and M. G. Betts. 2017. Assembly dynamics of a forest bird community depend on disturbance intensity and foraging guild. *Journal of Applied Ecology* 54:784-793. <https://doi.org/10.1111/1365-2664.12773>

Langham, G. M., J. G. Schuetz, T. Distler, C. U. Soykan, and C. Wilsey. 2015. Conservation status of North American birds in the face of future climate change. *PLoS ONE* 10: e0135350. <https://doi.org/10.1371/journal.pone.0135350>

Lehikoinen, A., and R. Virkkala. 2016. North by north-west: climate change and directions of density shifts in birds. *Global Change Biology* 22:1121-1129. <https://doi.org/10.1111/gcb.13150>

López-Segoviano, G., M. Arenas-Navarro, E. Vega, and M. Arizmendi. 2018. Hummingbird migration and flowering synchrony in the temperate forests of northwestern Mexico. *PeerJ* 6: e5131. <https://doi.org/10.7717/peerj.5131>

Mola, J. M., and N. M. Williams. 2018. Fire-induced change in floral abundance, density, and phenology benefits bumble bee foragers. *Ecosphere* 9: e02056. <https://doi.org/10.1002/ecs2.2056>

Møller, A. P. 2013. Long-term trends in wind speed, insect abundance and ecology of an insectivorous bird. *Ecosphere* 4(1): 6. <https://doi.org/10.1890/ES12-00310.1>

Momberg, M., D. W. Hedding, M. Luoto, and P. C. le Roux. 2021. Species differ in their responses to wind: the underexplored link between species fine-scale occurrences and variation in wind stress. *Journal of Vegetation Science* 32: e13093. <https://doi.org/10.1111/jvs.13093>

Moran, A., and D. F. Fraser. 2015. Rufous Hummingbird. In P. J. A. Davidson, R. J. Cannings, A. R. Couturier, D. Lepage, and C. M. Di Corrado, editors. *The atlas of the breeding birds of British Columbia, 2008-2012*. Bird Studies Canada, Delta, British Columbia, USA. <http://www.birdatlas.bc.ca/accounts/speciesaccount.jsp?sp=RUHU&lang=en>

Moran, A. J., S. W. J. Prosser, and J. A. Moran. 2019. DNA metabarcoding allows non-invasive identification of arthropod prey provisioned to nestling Rufous hummingbirds (*Selasphorus rufus*). *PeerJ* 7: e6596. <https://doi.org/10.7717/peerj.6596>

Mote, P. W., J. T. Abatzoglou, and K. E. Kunkel. 2013. Climate. Pages 25-40 in M. M. Dalton, P. W. Mote, and A. K. Snover, editors. *Climate change in the Northwest: implications for our landscapes, waters, and communities*. National Climate Assessment (NCA) Regional Input Reports, Island Press/Center for Resource Economics, Washington, D.C., USA. https://doi.org/10.5822/978-1-61091-512-0_2

Negrón-Juárez, R. I., J. A. Holm, B. Faybushenko, D. Magnabosco-Marra, R. A. Fisher, J. K. Shuman, A. C. de Araujo, W. J. Riley, and J. Q. Chambers. 2020. Landsat near-infrared (NIR) band and ELM-FATES sensitivity to forest disturbances and regrowth in the Central Amazon. *Biogeosciences* 17:6185-6205. <https://doi.org/10.5194/bg-17-6185-2020>

Oeser, J., M. Heurich, C. Senf, D. Pflugmacher, E. Belotti, and T. Kuemmerle. 2020. Habitat metrics based on multi-temporal Landsat imagery for mapping large mammal habitat. *Remote Sensing in Ecology and Conservation* 6:52-69. <https://doi.org/10.1002/rse2.122>

Patuxent Wildlife Research Center. 1999. Breeding bird survey route locations for lower 48 states, 1966-1998. National Atlas of the United States, Reston, Virginia, USA. <http://purl.stanford.edu/vy474dv5024>

Phalan, B. T., J. M. Northrup, Z. Yang, R. L. Deal, J. S. Rousseau, T. A. Spies, and M. G. Betts. 2019. Impacts of the Northwest Forest Plan on forest composition and bird populations. *Proceedings of the National Academy of Sciences, USA* 116:3322-3327. <https://doi.org/10.1073/pnas.1813072116>

Prieto-Torres, D. A., L. E. Nuñez Rosas, D. Remolina Figueroa, and M. del Coro Arizmendi. 2021. Most Mexican hummingbirds lose under climate and land-use change: long-term conservation implications. *Perspectives in Ecology and Conservation* 19:487-499. <https://doi.org/10.1016/j.pecon.2021.07.001>

Robinson, W. D., T. A. Hallman, and J. R. Curtis. 2020a. Benchmarking the avian diversity of Oregon in an era of rapid change. *Northwestern Naturalist* 101(3):180-193. <https://doi.org/10.1898/1051-1733-101.3.180>

Robinson, O. J., V. Ruiz-Gutierrez, and D. Fink. 2018. Correcting for bias in distribution modelling for rare species using citizen science data. *Diversity and Distributions* 24:460-472. <https://doi.org/10.1111/ddi.12698>

Robinson, O. J., V. Ruiz-Gutierrez, M. D. Reynolds, G. H. Golet, M. Strimas-Mackey, and D. Fink. 2020b. Integrating citizen science data with expert surveys increases accuracy and spatial extent of species distribution models. *Diversity and Distributions* 26:976-986. <https://doi.org/10.1111/ddi.13068>

Rosenberg, K. V., A. M. Dokter, P. J. Blancher, J. R. Sauer, A. C. Smith, P. A. Smith, J. C. Stanton, A. Panjabi, L. Helft, M. Parr, and P. P. Marra. 2019. Decline of the North American avifauna. *Science* 366:120-124. <https://doi.org/10.1126/science.aaw1313>

Rousseau, J., J. Alexander, and M. Betts. 2020. Using continental-scale bird banding data to estimate demographic migratory patterns for Rufous Hummingbird (*Selasphorus rufus*). *Avian Conservation and Ecology* 15(2): 2. <https://doi.org/10.5751/ACE-01612-150202>

Roy, D. P., V. Kovalevskyy, H. K. Zhang, E. F. Vermote, L. Yan, S. S. Kumar, and A. Egorov. 2016. Characterization of Landsat-7 to Landsat-8 reflective wavelength and normalized difference vegetation index continuity. *Remote Sensing of Environment* 185:57-70. <https://doi.org/10.1016/j.rse.2015.12.024>

Sauer, J. R., and W. A. Link. 2011. Analysis of the North American breeding bird survey using hierarchical models. *Auk* 128:87-98. <https://doi.org/10.1525/auk.2010.09220>

Schieck, J., and S. J. Song. 2006. Changes in bird communities throughout succession following fire and harvest in boreal forests of western North America: literature review and meta-analyses. *Canadian Journal of Forest Research* 36:1299-1318. <https://doi.org/10.1139/x06-017>

Şekercioğlu, C. H., G. C. Daily, and P. R. Ehrlich. 2004. Ecosystem consequences of bird declines. *Proceedings of the National Academy of Sciences* 101:18042-18047. <https://doi.org/10.1073/pnas.0408049101>

Shirley, S. M., Z. Yang, R. A. Hutchinson, J. D. Alexander, K. McGarigal, and M. G. Betts. 2013. Species distribution modelling for the people: unclassified Landsat TM imagery predicts bird occurrence at fine resolutions. *Diversity and Distributions* 19:855-866. <https://doi.org/10.1111/ddi.12093>

Sodhi, N. S., L. H. Liow, and F. A. Bazzaz. 2004. Avian extinctions from tropical and subtropical forests. *Annual Review of Ecology, Evolution, and Systematics* 35(1):323-345. <https://doi.org/10.1146/annurev.ecolsys.35.112202.130209>

Steen, V. A., M. W. Tingley, P. W. C. Paton, and C. S. Elphick. 2021. Spatial thinning and class balancing: key choices lead to variation in the performance of species distribution models with citizen science data. *Methods in Ecology and Evolution* 12:216-226. <https://doi.org/10.1111/2041-210X.13525>

Strimas-Mackey, M., W. M. Hochachka, V. Ruiz-Gutierrez, O. J. Robinson, E. T. Miller, T. Auer, S. Kelling, D. Fink, and A. Johnston. 2020. Best practices for using eBird data. Version 1.0. Cornell Lab of Ornithology, Ithaca, New York, USA. <https://doi.org/10.5281/zenodo.3620739>

Svetnik, V., A. Liaw, C. Tong, J. C. Culberson, R. P. Sheridan, and B. P. Feuston. 2003. Random forest: a classification and regression tool for compound classification and QSAR modeling. *Journal of Chemical Information and Computer Sciences* 43:1947-1958. <https://doi.org/10.1021/ci034160g>

Thomas, C. D., and J. J. Lennon. 1999. Birds extend their ranges northwards. *Nature* 399:213-213. <https://doi.org/10.1038/20335>

Thomas, J.W., J. F. Franklin, J. Gordon, and K. N. Johnson. 2006. The Northwest forest plan: origins, components, implementation experience, and suggestions for change. *Conservation Biology* 20:277-287. <https://doi.org/10.1111/j.1523-1739.2006.00385.x>

Tracewski, L., S. H. M. Butchart, M. Di Marco, G. F. Ficetola, C. Rondinini, A. Symes, H. Wheatley, A. E. Beresford, and G. M. Buchanan. 2016. Toward quantification of the impact of 21st-century deforestation on the extinction risk of terrestrial vertebrates. *Conservation Biology* 30:1070-1079. <https://doi.org/10.1111/cobi.12715>

Trautmann, S. 2018. Climate change impacts on bird species. Pages 217-234 in D. T. Tietze, editor. *Bird species: how they arise, modify and vanish*. Fascinating Life Sciences, Springer International Publishing, Dordrecht, The Netherlands. https://doi.org/10.1007/978-3-319-91689-7_12

Vásquez-Aguilar, A. A., J. F. Ornelas, F. Rodríguez-Gómez, and M. C. MacSwiney González. 2021. Modeling future potential distribution of Buff-Bellied Hummingbird (*Amazilia yucatanensis*) under climate change: species vs. subspecies. *Tropical Conservation Science* 14: 19400829211030834. <https://doi.org/10.1177/19400829211030834>

Vila-Viçosa, C., S. Arenas-Castro, B. Marcos, J. Honrado, C. García, F. M. Vázquez, R. Almeida, and J. Gonçalves. 2020. Combining satellite remote sensing and climate data in species distribution models to improve the conservation of Iberian white oaks (*Quercus* L.). *International Journal of Geo-Information* 9: 735. <https://doi.org/10.3390/ijgi9120735>

Vose, R. S., D. R. Easterling, K. E. Kunkel, A. N. LeGrande, and M. F. Wehner. 2017. Temperature changes in the United States. Pages 185-206 in D. J. Wuebbles, D. W. Fahey, K. A. Hibbard, D. J. Dokken, B. C. Stewart, and T. K. Maycock, editors. *Climate science special report: fourth national climate assessment, volume I*. U.S. Global Change Research Program, Washington, D.C., USA.

Wickham, J., A. Neale, K. Riitters, M. Nash, J. Dewitz, S. Jin, M. van Fossen, and D. Rosenbaum. 2023. Where forest may not return in the western United States. *Ecological Indicators* 146: 109756. <https://doi.org/10.1016/j.ecolind.2022.109756>

Appendix 1

Multicollinearity of covariates

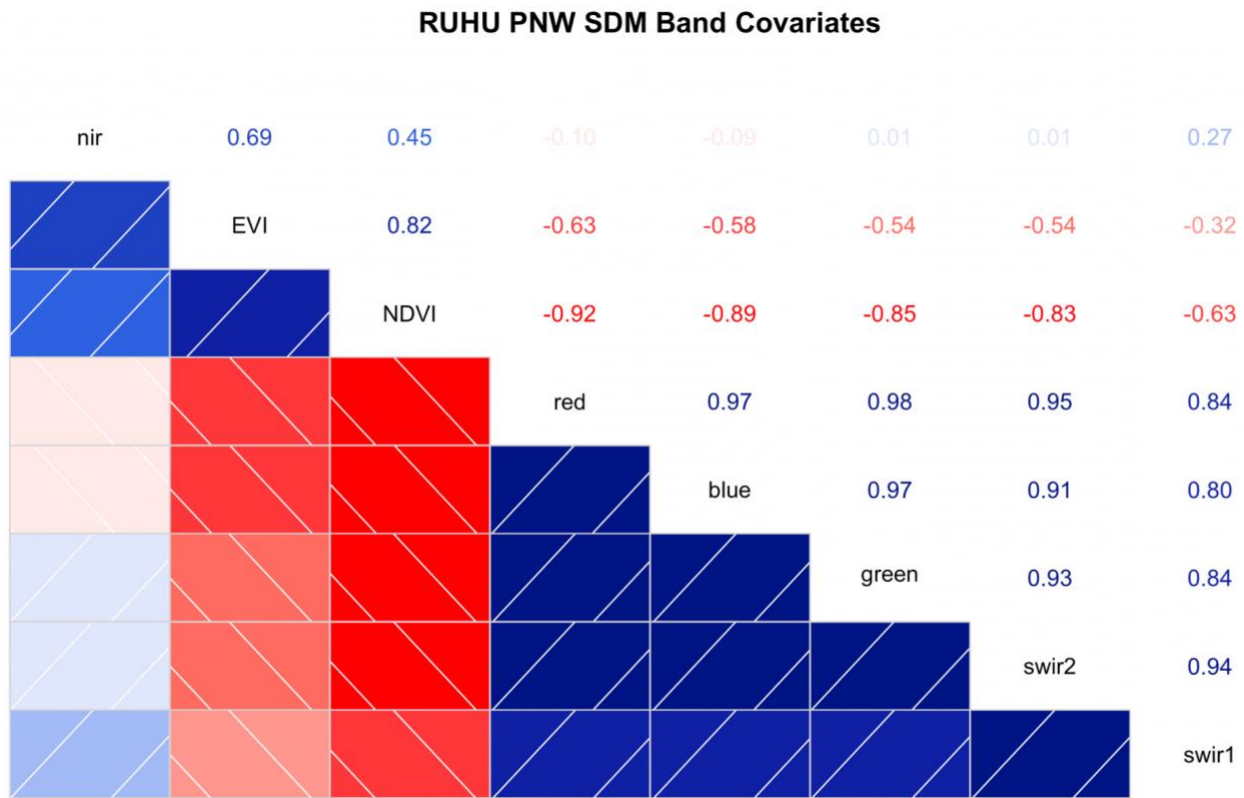


Fig. S1.1 Correlation matrix of all spectral bands considered for model prediction. Correlations were run using a Pearson correlation test using the “corrgram” package in R. All of the spectral reflectance bands and vegetation indices were highly correlated with the exception of near-infrared reflectance.

RUHU PNW SDM Climate Covariates

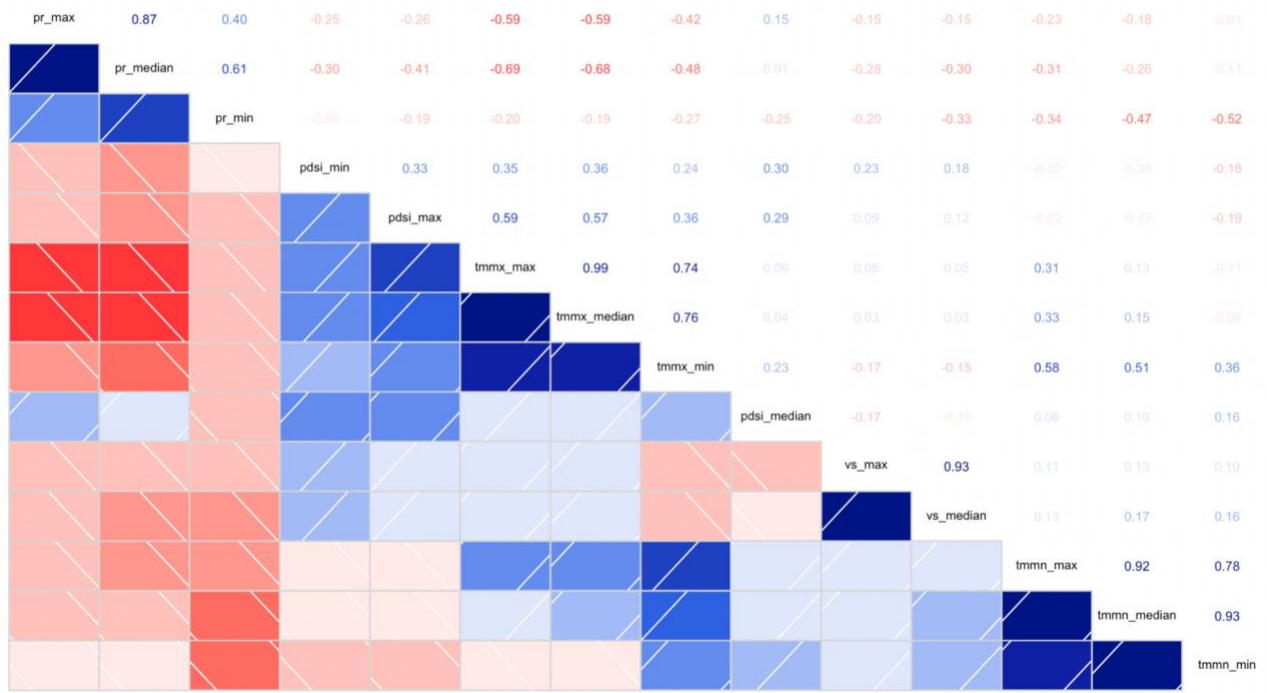


Fig. S1.2 Correlation matrix of all climate variables considered for model prediction.

Correlations were run using a Pearson correlation test using the “corrgram” package in R. Because summer median maximum temperature (‘tmmx_median’) was highly correlated (Pearson’s r greater than 0.65) with median precipitation accumulation (‘pr_median’), we selected the median Palmer Drought Severity Index (‘pdsi_median’).

RUHU PNW SDM Selected Covariates



Fig. S1.3 Correlation matrix of climate and remote sensing variables selected as model predictors. Correlations were run using a Pearson correlation test using the “corrgram” package in R. None of the selected predictors exhibit collinearity.

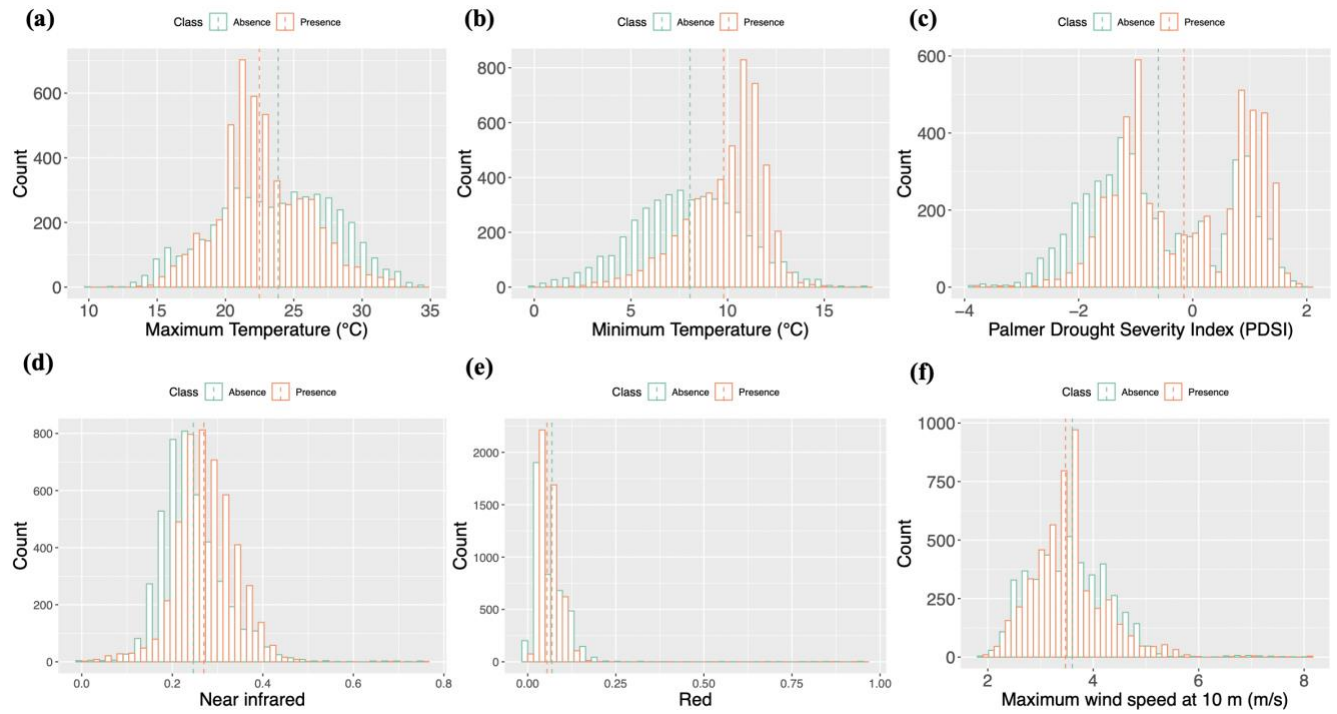


Fig. S1.4 Histograms of predictor values for all Rufous Hummingbird presence points (blue, Class = 'TRUE') and absence points (red, Class = 'FALSE'). Covariate values were calculated as the summer median in the 250m pixel around the presence or absence point. **(a)** Rufous Hummingbird presence points have a lower mean maximum temperature (22.4 °C) compared to absence points (23.8°C). **(b)** Presence points have a higher mean minimum temperature (9.8 °C) compared to absence points (8.1°C). **(c)** Presence points have a higher mean PDSI value (-0.15) compared to absence points (-0.60), indicating that Rufous Hummingbirds are more likely to be present in moist conditions. The PDSI estimates relative dryness based on temperature and precipitation data; values range from -4 to 4, with -4 indicating severe drought and +4 indicating an extreme moist spell. Note the lack of presences with PDSI values -2 or lower (moderate drought). **(d)** Presence points have a lower mean red surface reflectance (0.055) compared to absence points (0.069). **(e)** Presence points have a higher mean near-infrared surface reflectance (0.27) compared to absence points (0.24). **(f)** Presence points have lower mean maximum wind-speed values (3.47 m/s) compared to absence points (3.60 m/s).

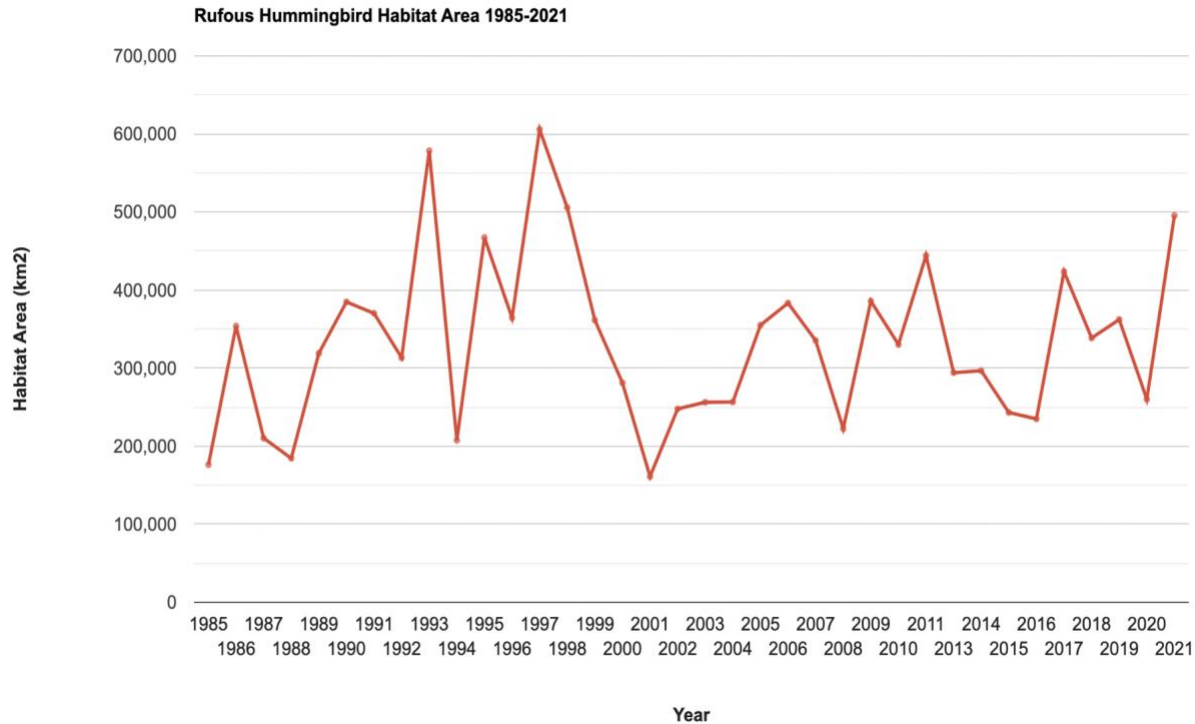


Fig. S1.5 Yearly area of suitable RUHU habitat predicted by our SDM from 1985–2021. Area amounts were calculated by masking yearly habitat suitability images with the mean classification threshold that maximized the sum of sensitivity and specificity (habitat suitability > 0.42). Note that high variability in RUHU habitat area in the 1990s, coinciding with substantial changes to forest management during the 90s in the PNW under the passage of the 1994 Northwest Forest Plan.

Table S1 Accuracy metrics for each of the 10 model runs including average values (avg) for area under the curve evaluation (AUCROC), true skill statistic (TSS), false positive rate (FPR), and false negative rate (FNR).

Model run	FN	FP	FPR	Precision	SUMSS	TN	TNR	TP	TPR	cutoff	TSS	FNR	AUCROC
0	325	181	0.24	0.88	1.56	586.00	0.76	1288.00	0.80	0.50	0.56	0.20	0.85
1	242	85	0.15	0.91	1.63	499.00	0.85	830.00	0.77	0.63	0.63	0.23	0.80
2	314	184	0.23	0.77	1.44	617.00	0.77	628.00	0.67	0.46	0.44	0.33	0.78
3	153	319	0.33	0.54	1.38	647.00	0.67	373.00	0.71	0.25	0.38	0.29	0.77
4	118	360	0.45	0.55	1.34	443.00	0.55	445.00	0.79	0.33	0.34	0.21	0.81
5	411	261	0.19	0.85	1.59	1094.00	0.81	1456.00	0.78	0.46	0.59	0.22	0.81
6	56	344	0.47	0.45	1.37	392.00	0.53	281.00	0.83	0.25	0.37	0.17	0.83
7	64	141	0.26	0.53	1.45	402.00	0.74	157.00	0.71	0.38	0.45	0.29	0.86
8	68	222	0.34	0.56	1.46	433.00	0.66	277.00	0.80	0.29	0.46	0.20	0.83
9	83	101	0.25	0.74	1.53	304.00	0.75	286.00	0.78	0.46	0.53	0.22	0.78
avg			0.29								0.47	0.24	0.81

Appendix 2

Model structure

The model is a relatively simple, hierarchical log-link negative binomial regression, like other models commonly applied to the BBS [Sauer and Link (2011)](Smith et al. 2014), except applied at the route-level instead of pooling routes into geographic strata e.g., (Betts et al. 2022). In this model, each route has a separate slope and intercept and there are no annual intercepts to model annual or non-linear temporal patterns in population change. Therefore, the interpretation of “trend” in these models is limited to a log-linear slope parameter.

$$C_{r,j,t} = \text{Negative Binomial}(\lambda_{r,j,t}, \phi)$$

$$\log(\lambda_{r,j,t}) = \alpha_r + \beta_r * (t - t_m) + \eta I[j, t] + \omega_j$$

We modeled the observed counts ($C_{r,j,t}$) of Rufous Hummingbirds on route-r, in year-t, by observer-j as realizations of a negative binomial distribution, with mean $\lambda_{r,j,t}$ and inverse dispersion parameter ϕ . The log of the mean ($\lambda_{r,j,t}$) of the negative binomial distribution was modeled as an additive combination of route-level intercepts (α_r), observer-effects (ω_j), and a first-year observer-effect ($\eta I[j, t]$), and route-level slope parameters (β_r) for the continuous effect of year (t) centered on the mid-year of the time-series (t_m).

We estimated the the first-year observer-effect η , as an independent parameter with weakly informative prior (below). All other parameters were estimated as hierarchical-effects, sharing information among routes or among observers.

We estimated the route-level intercepts and slopes as an additive combination of a mean species-level intercept or slope (α' or β'), a varying intercept or slope that was a function of the mean habitat suitability on the route (α''_r) or rate of change in habitat suitability on the slope (β''_r), and spatially varying effects for the remaining variation in relative abundance (α'''_r) and slope (β'''_r) that were not explained by habitat.

$$\alpha_r = \alpha' + \alpha''_r + \alpha'''_r$$

We estimated the effect of mean habitat suitability on the route-level intercept as a simple product of a route-specific coefficient (ρ_{α_r}) and the average of the annual habitat suitabilities in a buffer surrounding each route-path ($\alpha''_r = \rho_{\alpha_r} * \mu_{habitsuitability_r}$). We estimated the effect of the rate of change in habitat suitability over time on the route-level slope as a product of a route-specific coefficient (ρ_{β_r}) and an estimate of the average rate of change in habitat suitability on each route ($\delta_{habitsuitability_r}$), calculated using a simple linear regression through the annual estimates of habitat suitability in a buffer surrounding each route-path ($\beta''_r = \rho_{\beta_r} * \delta_{habitsuitability_r}$). The habitat suitability predictors were standardized (both centered and scaled) to improve convergence. The route-specific coefficients for the effects of habitat suitability on the intercept and slope were allowed to vary among routes, but were centered on a hyperparameter mean effects across routes $\rho_{\alpha_r} \sim Normal(P_\alpha, \sigma_{\rho_\alpha})$ and $\rho_{\beta_r} \sim Normal(P_\beta, \sigma_{\rho_\beta})$. As such, the hyperparameters for the effect of mean habitat suitability on the intercept (P_α) and the effect of change in habitat suitability on slope (P_β), represent a clear species-level estimate of the overall effects of habitat on abundance and trend, after adjusting for the species mean abundance and trend, as well as the residual spatially dependent variation in abundance and trend.

In the fully spatial implementation of the model, we estimated the residual component of the intercepts and slopes using an intrinsic iCAR structure, where the parameter for route- r is drawn from a normal distribution, centered on the mean of that parameter's values in all neighbouring routes, with an estimated standard deviation that is proportional to the inverse of the number of neighbours for that route(Morris et al. 2019). Specifically, the component of the intercept that represents the residual spatially dependent relative abundance (α'''_r) was drawn from a normal distribution centered on the mean of the intercepts for all neighbouring routes.

$$\alpha'''_r \sim Normal\left(\frac{\sum_{n \in N_r} \alpha'''_n}{N_r}, \frac{\sigma_{\alpha'''}}{N_r}\right)$$

The spatially varying component of the slope (β'''_r) was estimated similarly as random route-level terms from a normal distribution centered on the mean of the slopes for all neighbouring routes using the same iCAR structure.

$$\beta'''_r \sim Normal\left(\frac{\sum_{n \in N_r} \beta'''_n}{N_r}, \frac{\sigma_{\beta'''}}{N_r}\right)$$

Alternative non-spatial residual term on intercepts

For both time-periods, there was a relatively strong spatial autocorrelation in both the habitat suitability and the mean abundance of the species. Since the spatial component of habitat suitability could reasonably be considered as a cause of the spatial dependency in abundance,

we drew our final inference on the effect of habitat suitability on abundance from a model that estimated the residual component of the intercept term with a non-spatial varying effect (i.e., a simple random effect). Specifically, the component of the intercept that represents the residual relative abundance (α_r''') was drawn from a normal distribution centered at zero with an estimated standard deviation ($\alpha_r''' \sim \text{Normal}(0, \sigma_{\alpha''''})$).

Spatial components

In other work, we have fit models with two different approaches to modeling the spatially explicit relationships among routes: a Gaussian process (GP) model that uses a matrix of Euclidian distances separating the start-locations of each BBS route, treating distance between routes as a continuous measure; and 2) an intrinsic Conditional Autoregressive (iCAR) structure that uses a sparse matrix of adjacencies between pairs of routes based on a tessellation of the intervening space, treating spatial relationships as a series of discrete neighbours. Because the observations from a given BBS route are collected along a transect that is approximately 40km in length, it is not obvious which treatment of the spatial relationships better reflects reality. Spatial models are well developed for data collected at points and for data collected within discrete areas (Pebesma and Bivand 2023), but the BBS transects are neither points nor areas. Our prior work has shown that for route-level models of BBS data, the GP and iCAR approaches result in almost identical predictions, but the iCAR approach is much less computationally demanding (models fit in minutes rather than hours or days).

Both of these approaches are simplifications of the true spatial relationships among the BBS routes. The GP approach simplifies the spatial relationships by assuming each route represents a point in space and ensures that the covariance between pairs of routes declines with distance, but that measure of intervening distance only applies to the distances between the start points of the routes, not to the full transect. The iCAR approach simplifies the spatial structure by assuming each route represents a discrete area of space (a polygon surrounding the route), but the neighbouring routes may be separated by a wide range of distances depending on the spatial distribution and spatial density of those routes. For example, the GP could consider two distant routes as effectively independent, irrespective of how many routes were located in the intervening space. By contrast, the iCAR structure could consider these same two routes as having a very close connection if there were no intervening routes. In some cases, treating two relatively distant routes as close neighbours may be useful if their relative proximity provides useful information to inform the parameter estimates but may also introduce error into the estimate of spatial variance by considering the relatively distant neighbours as similar to relatively close neighbours.

The iCAR spatial structures require a discrete representation of spatial neighbourhood relationships (Ver Hoef et al. 2018), we used a Voronoi tessellation to generate these discrete neighbourhood relationships (Pebesma and Bivand 2023). iCAR models are often applied to contiguous areal stratifications, such as regular grids, census regions, or political jurisdictions, which have natural neighbourhood relationships defined by their adjacencies [Ver Hoef

et al. (2018)](Meehan et al. 2019). To generate contiguous discrete spatial units without imposing a regular grid structure, we created a Voronoi tessellation centered on the start points of each BBS route (Pebesma 2018). We further limited the adjacency matrix to the approximate boundaries of the species' range, by clipping the tessellated surface using the standard BBS analytical strata where the species occurs (province/states intersected with the Bird Conservation Regions; (Link and Sauer 2002) and a concave polygon surrounding the route start locations (Gombin et al. 2020). This clipping ensured that adjacency relationships did not extend beyond the borders of the species' range, and allowed the adjacency matrix to respect large-scale complex range boundaries. Within the species' range boundaries, routes were considered neighbours if their Voronoi polygon shared a linear segment along a separating boundary. Our approach to generating these adjacency relationships may introduce variance, because some neighbouring routes may be much further apart than others. However, it is sufficiently flexible to ensure a comprehensive and contiguous network of among-route links, and accurately represents the relative spatial adjacencies (each route is considered adjacent to its nearest neighbours) if not always the true Euclidean space.

Fitting the model

The model assumes that population trends at a given route can be reasonably described using a continuous log-linear slope parameter. This assumption of *trend* as an average rate of change across the entire time-series is probably most reasonable for relatively short periods of time (e.g., 10-20 years). For longer periods of time it is likely that natural populations will follow some more complex, non-linear path and therefore that the assumption of a continuous rate of change in the population over the full time-series is less likely (Smith and Edwards 2020). Indeed, for Rufous Hummingbird populations in North America appear to show a break point in the population trend in approximately 2005. Between 1985 and 2005, the continental population was relatively stable, and after 2005 it declined steeply. To account for this nonlinearity in the population trajectory, we fit the model separately for the 20-year period from 1985-2005 and for the 15-year period from 2006-2021.

Before fitting the model, we prepared the BBS counts, the neighbourhood structures necessary to estimate the iCAR residual spatial component, and joined them to the habitat suitability predictors. The full code and data necessary to replicate the data-preparation is available in the online supplement. In brief, we selected all routes on which the species had been observed during the time-period (1985-2005 or 2006-2021), and for which we had GIS route-path information that would allow us to estimate the route-specific annual habitat suitability values.

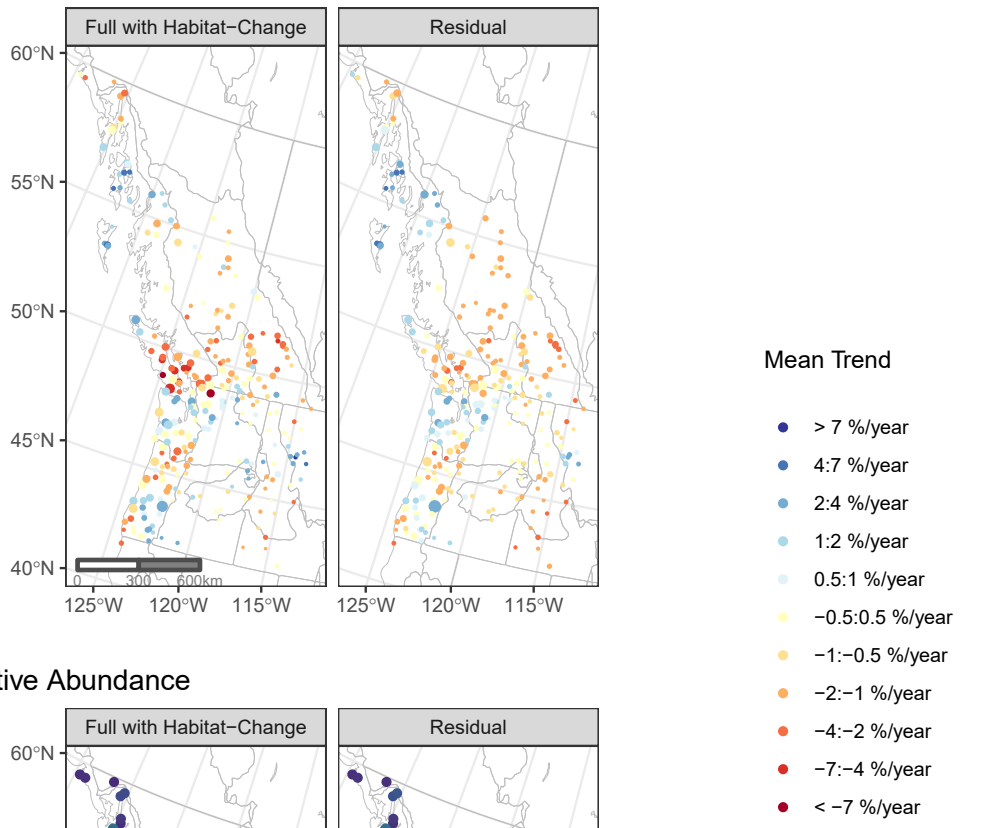
We fit the model using the probabilistic programming language Stan (Stan Development Team 2022), accessed through the R-package `cmdstanr` (Gabry and Cešnovar 2022). We used a warm-up of 2000 iterations, and `cmdstanr` default settings for other arguments, followed by a draw of 2000 samples from which we estimated the posterior distributions. All parameters in all models converged based on $Rhat < 1.02$ and bulk effective sample sizes > 500 .

Results

1985-2005

During the first 20 years from 1985-2005, the species overall population was generally stable. The model estimated an overall change in the population of approximately -11% [-27:5.5]. Trends varied among routes and regions (Figure S2.1). The effect of habitat on mean relative abundance was strong and positive ($P_\alpha = 3.1$ [2.3:4]), if the residual trend was modeled without the spatial-dependency. However, when the spatial dependency was included, most of the variation in the relative abundance was allocated to the spatial component. There was a positive effect of change in the habitat suitability on trends, such that routes with habitat-loss had more negative population trends. However, this effect was somewhat uncertain $P_\beta = 0.05$ [-0.011:0.11], and 0 was included within the 95% posterior credible interval.

Trend



Relative Abundance

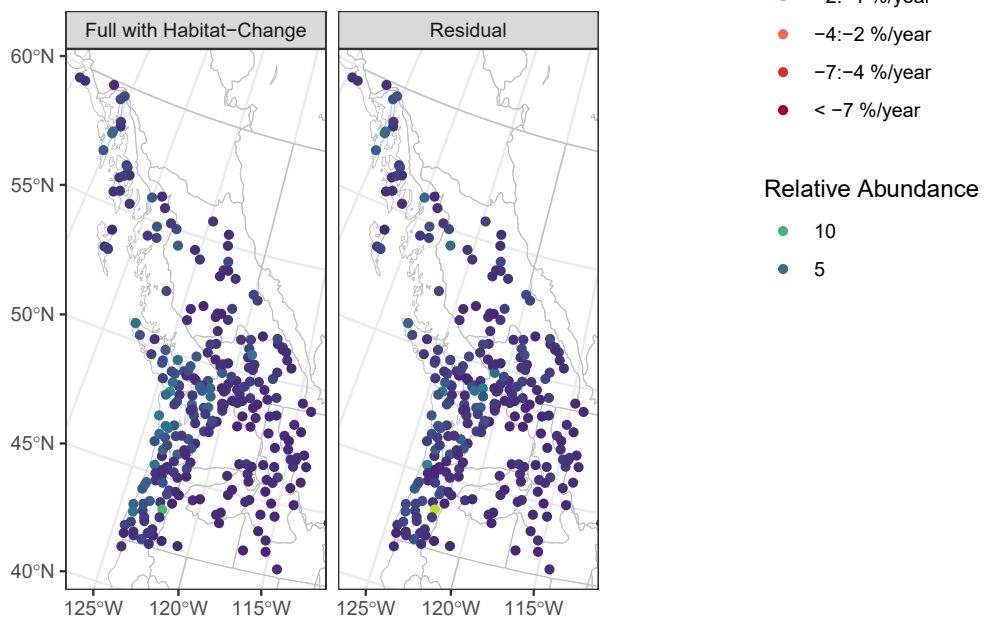
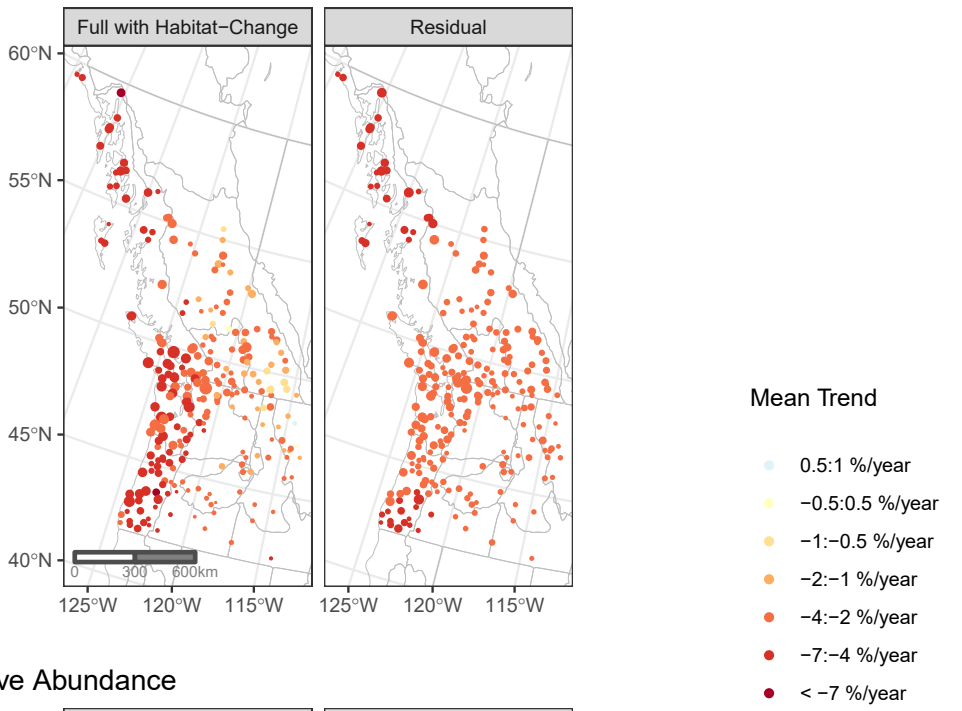


Figure 1: Map of the trends for Rufous Hummingbird from 1985-2005. The colours represent the trends in the upper panel and the relative abundance in the lower panel. The left panel represents the full estimated trends and abundance on each route, including both the effect of habitat-suitability and the residual component not related to habitat. The right panel represents the trends and relative abundances after removing the effect of habitat-suitability. In the top-left panel, the greater declines in central-coastal regions are evident from the darker red points compared to the top-right panel. In the bottom-left panel, the higher abundance near the coast is evident from the lighter colours. The bottom-right panel shows much more even relative abundance across the species' range, showing that habitat suitability accounts for much of the variation in abundance. Spatial extent and location within western North America, is the same as Figure 4 in the main paper.

2006-2021

During the later 15 years from 2006-2021, the species overall population declined steeply. The model estimated an overall change in the population of approximately -43% [-52:-33]. Trends were negative across the species' range, but most negative in the coastal regions where the species is also most abundant (Figure S2.2). The effect of habitat suitability on mean relative abundance was strong and positive ($P_\alpha = 3$ [2.2:3.8]), and this effect was robust, whether the residual abundance component was spatially autocorrellated or random. There was a clear positive effect of change in the habitat suitability on trends, such that routes with habitat-loss had more negative population trends $P_\beta = 0.025$ [0.0022:0.047]. The greater loss of habitat in the coastal region accounts for most of the increased rates of decline in that region (Figure S2.2), the residual trend component alone (Figure S2.2, right panel) does not show the same coastal-decline pattern.

Trend



Relative Abundance

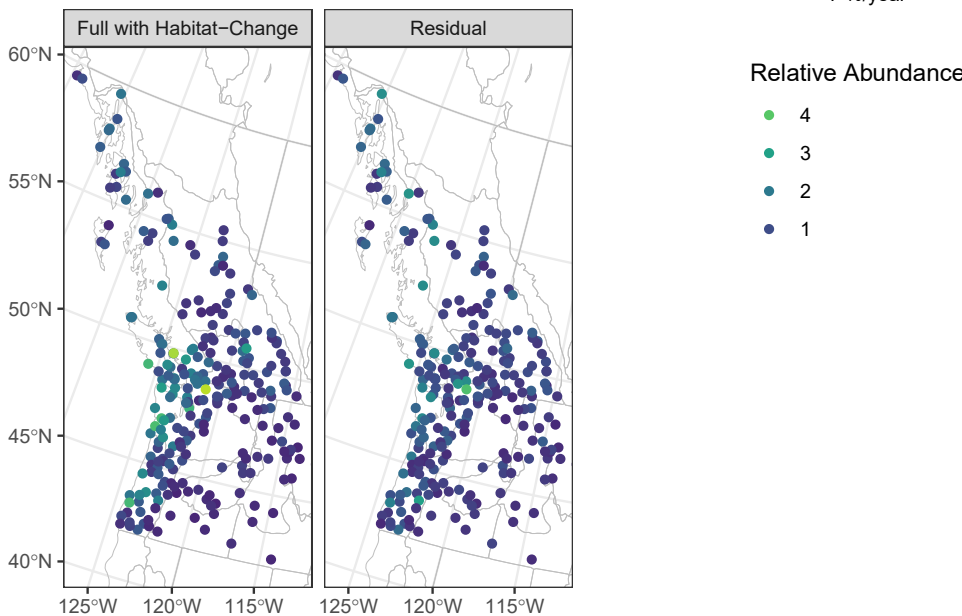


Figure 2: Map of the trends for Rufous Hummingbird from 2006-2021. The colours represent the trends in the upper panel and the relative abundance in the lower panel. The left panel represents the full estimated trends and abundance on each route, including both the effect of habitat-suitability and the residual component not related to habitat. The right panel represents the trends and relative abundances after removing the effect of habitat-suitability.⁸ In the top-left panel, the greater declines in coastal regions are evident from the darker red points compared to the top-right panel. In the bottom-left panel, the higher abundance near the coast is evident from the lighter colours. The bottom-right panel shows much more even relative abundance across the species' range, showing that habitat suitability accounts for much of the variation in abundance. Spatial extent and location within western North America, is the same as Figure 4 in the main paper.

References

Betts, M. G., Z. Yang, A. S. Hadley, A. C. Smith, J. S. Rousseau, J. M. Northrup, J. J. Nocera, N. Gorelick, and B. D. Gerber. 2022. Forest degradation drives widespread avian habitat and population declines. *Nature Ecology & Evolution* 6:709–719. <https://doi.org/10.1038/s41559-022-01737-8>.

Gabry, J., and R. Cešnovar. 2022. *Cmdstanr: R interface to 'CmdStan'*.

Gombin, J., R. Vaidyanathan, and V. Agafonkin. 2020. *Concaveman: A very fast 2D concave hull algorithm*.

Link, W. A., and J. R. Sauer. 2002. A Hierarchical Analysis of Population Change with Application to Cerulean Warblers. *Ecology* 83:2832–2840. [https://doi.org/10.1890/0012-9658\(2002\)083%5B2832:AHAOPC%5D2.0.CO;2](https://doi.org/10.1890/0012-9658(2002)083%5B2832:AHAOPC%5D2.0.CO;2).

Meehan, T. D., N. L. Michel, and H. Rue. 2019. Spatial modeling of Audubon Christmas Bird Counts reveals fine-scale patterns and drivers of relative abundance trends. *Ecosphere* 10:e02707. [https://doi.org/https://doi.org/10.1002/ecs2.2707](https://doi.org/10.1002/ecs2.2707).

Morris, M., K. Wheeler-Martin, D. Simpson, S. J. Mooney, A. Gelman, and C. DiMaggio. 2019. Bayesian hierarchical spatial models: Implementing the Besag York Mollié model in stan. *Spatial and Spatio-temporal Epidemiology* 31:100301. <https://doi.org/10.1016/j.sste.2019.100301>.

Pebesma, E. 2018. *Simple Features for R: Standardized Support for Spatial Vector Data*. The R Journal 10:439–446.

Pebesma, E., and R. Bivand. 2023. *Spatial Data Science: With Applications in R*, 1st edition. Chapman; Hall/CRC, Boca Raton. <https://doi.org/10.1201/9780429459016>.

Sauer, J. R., and W. A. Link. 2011. Analysis of the North American Breeding Bird Survey Using Hierarchical Models. *The Auk* 128:87–98. <https://doi.org/10.1525/auk.2010.09220>.

Smith, A. C., and B. P. M. Edwards. 2020. North american breeding bird survey status and trend estimates to inform a wide range of conservation needs, using a flexible bayesian hierarchical generalized additive model. *The Condor*. <https://doi.org/10.1093/ornithapp/duaa065>.

Smith, A. C., M.-A. R. Hudson, C. Downes, and C. M. Francis. 2014. Estimating breeding bird survey trends and annual indices for Canada: how do the new hierarchical Bayesian estimates differ from previous estimates? *The Canadian Field-Naturalist* 128:119–134. <https://doi.org/10.22621/cfn.v128i2.1565>.

Stan Development Team, 2. 29. 2022. *Stan modeling language users guide and reference manual*.

Ver Hoef, J. M., E. E. Peterson, M. B. Hooten, E. M. Hanks, and M.-J. Fortin. 2018. Spatial autoregressive models for statistical inference from ecological data. *Ecological Monographs* 88:36–59. <https://doi.org/10.1002/ecm.1283>.